ABSTRACT

Total Electron Scattering Cross Sections of Ethane, Propane, n-Butane, 1,3-Butadiene and Butylene in the Energy Range 0.3 to 4.0 keV

Priyangika Wickramarachchi

Mentor: Wickramasinghe Ariyasinghe, Ph.D.

The total electron scattering cross sections of Ethane, Propane, n-Butane, 1,3-Butadiene and Butylene were measured in the energy range 0.3 to 4.0 keV using linear transmission technique. The measured experimental cross sections were compared to the cross sections obtained by several experimental and theoretical groups. A simple empirical formula was developed by analyzing experimental cross sections to predict the cross sections of alkanes. This formula contains the number of carbon and hydrogen atoms in the molecule as well as the energy of electrons. Formula reproduces the total electron scattering cross sections in the range of 0.3 to 4.0 keV. The cross sections obtained from the empirical formula are compared to the present experimental cross sections, other experimental cross sections and theoretical cross sections available in the literature.

Total Electron Scattering Cross Sections of Ethane, Propane, n-Butane, 1,3-Butadiene and Butylene in the Energy Range 0.3 to 4.0 keV

by

Priyangika Wickramarachchi

A Thesis

Approved by the Department of Physics

Gregory A. Benesh, Ph.D., Chairperson

Submitted to the Graduate Faculty of
Baylor University in Partial Fulfillment of the
Requirements for the Degree
of
Master of Science

Approved by the Thesis Committee

Wickramasinghe M. Ariyasinghe, Ph.D., Chairperson

Kenneth T. Park, Ph.D.

Dwight P. Russell, Ph.D.

Stephen L. Gipson, Ph.D.

Accepted by the Graduate School
December 2006

J. Larry Lyon, Ph.D., Dean

TABLE OF CONTENTS

LIST OF FIGURES

LIST OF TABLES

ACKNOWLEDGMENTS

The author would like to express her gratitude to her thesis supervisor and the chairman of the thesis committee, Dr. Ariyasinghe Wickramasinghe for his continuous support, guidance and encouragement throughout this work. I also appreciate his help in editing the thesis. The author would also like to thank Dr. K. Park, Dr. D. Russell and Dr. S. L.Gipson for their help and willingness to be the thesis committee members. My sincere appreciations go to the faculty and staff of the Department of Physics, Baylor University, for their kind support in many ways.

The author would like to dedicate this to her loving parents.

CHAPTER ONE

Introduction

1.1 Total Electron Scattering Cross Section

Total electron scattering cross section (TCS) of a medium describes the total probability of scattering an energetic electron as it penetrates through the medium. Therefore the total cross section is a measure of the effective surface area of the target molecules or atoms presented to the energetic electrons and it is expressed in the units of area. The knowledge of the effective surface area of a target material is important in many areas of pure and applied sciences. As a result, the study of electron scattering cross section of atoms and molecules has been a subject of intense research activity for almost a century [1]. First few decades of research in this area were confined mainly to low electron energies owing to the experimental difficulties at high energies and lack of interest for high energy cross sections in applications. Later, with the development of new experimental techniques to energetically analyze intermediate and high energy electrons, the interest was extended to the intermediate and high energy electrons. This development was further supported by the increased demand of cross sections for intermediate and high energy electrons in applied sciences.

This thesis will be devoted to the measurement of electron scattering cross section of five hydrocarbons at intermediate electron energies. In the first chapter, some of the applications will be discuss in detail stressing the importance of studying TCS of hydrocarbon molecules. Then, in the same chapter, the experimental and theoretical studies available in the literature which are related to the present work will be discussed.

The experimental technique used to determine the TCS will be explained in chapter two. The experimental results along with an analytical expression to reproduce these will be presented in chapter three. Finally, based on the experimental observations and empirical analysis in this work, a conclusion will be given in the last chapter.

1.2 Applications of Total Electron Scattering Cross Sections

The total cross sections of electron scattering from atoms and molecules are very important because of their applications in wide variety of fields in physics, chemistry, biology and medicine [2]. Astrophysics, plasma physics, planetary and atmospheric physics, and semiconductor physics are few common areas of physics where the cross sections are widely used [1]. In planetary and atmospheric physics electron scattering cross sections are used in modeling the composition of planetary atmosphere or the composition of the interstellar space. Microcircuit fabrications in semiconductor physics, electron scattering cross sections are used to understand the electrical discharges in microcircuits. It has been investigated that due to high energy electrons in biological degradation, radiation interacts with tissue and cellular structure. Therefore in biological systems, electron scattering cross sections are used in the determination of radiation damage and to understand the mammalian nervous systems and consciousness [2]. Apart from these practical applications, accurate experimental cross sections are used in the development of theoretical models to understand the energetic electron atom interaction process. Furthermore these cross sections are important in the development of empirical formulas for the predictions of penetrating depth of energetic electrons in gasses, liquids and solids. The knowledge of the electron scattering from hydrocarbon molecules is essential, due to important applications of these hydrocarbon compounds.

Some of the common areas where the TCS of hydrocarbons are used will be discussed next.

1.2.1 Atmospheric Physics (Earth and Other Planets)

In our solar system all planets have gaseous atmospheres which are continuously exposed to the solar radiation. In the ionosphere, solar radiation ionizes the atmospheric constituents. As a result of this ionization process energetic free electrons are produced in planetary atmospheres. When these electrons move through the atmospheric constituents, they lose their energy via several processes such as ionization, excitation and collision with ions and gas molecules. This energy loss is a measure of the production of ions and molecular fragments in the paths of energetic electrons. Therefore electron scattering cross sections are absolutely necessary tool in understanding these ionospheric processes occur in the upper atmosphere.

Aurora is one of the most interesting applications of electron molecule scattering. This phenomenon represents a relation between the solar radiation, magnetosphere and ionosphere of a planet. The ionization processes occur in the aurora are same as the ionospheric process explained above. The only difference is the main source for auroral process is highly energetic (~1- 10 keV) electrons which are emerging from the solar radiation. Therefore electron molecule scattering cross sections for higher energies are needed to understand the actual kinetic process behind the auroral phenomena.

Listed in Table 1.1 are the atmospheric constituents of different atmospheres of the planets in solar system. As can be seen from this table, ethane is one of the basic constituent of most planets except for Mars, Venus, Mercury and Earth. Other than ethane, there are certain amount of heavier hydrocarbon gases in the atmospheres of

major planets like Saturn and Jupiter. Therefore study of electron scattering cross section by hydrocarbon molecules will provide useful information to understand the atmospheric systems, aurora, airglow and lightening in the planetary atmospheres which contain hydrocarbon compounds.

Table 1.1 Components of various Planetary Atmospheres [1]

Planet	Components
Earth	N_2, O_2, H_2O, Ar , CO_2
Mercury	(H , He , O)?
Venus	Ar, N_2, HCl, HF, H_2O, CO_2, SO_2
Mars	Ne, Ar, Kr, Xe, N_2, O_2, CO, O_3, CO_2, H_2O
Jupiter	He, K, Na, H_2, CO, CO_2, H_2O, SO_2, HCN, NH_3, CH_4, C_2H_2, C_2H_6, PH_3, GeH_4
Saturn	He, H_2, CH_4, NH_3, C_2H_2, C_2H_6, C_3H_4, C_3H_8
Uranus	H_2, CH_4, (He, NH_3)?
Neptune	H_2, CH_4, (He, NH_3)?
Pluto	CH_4, (Ne)?

1.2.2 Plasma Processing

Electron collision processes are very important in both manmade and natural plasmas to determine the energy balances and transport properties of electrons. Hydrocarbons are commonly produced in manmade hydrogen plasmas. For example, carbon is commonly used for plasma walls in fusion devices because of its specific qualities. But for the hydrogen plasmas, carbon is problematic since there is a possibility for chemical sputtering. As a result, it releases significant amount of several hydrocarbon impurities ranging from CH_4 to C_3H_8, and it has been found that 50% of the total erosion of surface is due to these heavier hydrocarbons [3]. Therefore electron scattering cross

sections for hydrocarbon molecules are very useful to understand the reactions between these hydrocarbons and the background of hydrogen plasma.

Plasma etching, deposition and cleaning are essential fabrication methods in the manufacture of micro electronic components. Since most of the new plasma tools operate at low pressure and high plasma densities, the gasses which used for these processes are highly fragmented. It has been reported that in some cases feedstock gasses disassociate over 90% [4]. Therefore electron scattering cross sections and disassociation cross sections for fragments of these gasses are useful in the development of plasma equipments as well as in the understanding of the mechanisms of plasma processes. In particular, the cross section information of hydrocarbon molecules are the most important in this case because hydrocarbon compounds (*ie*. $C_xH_yF_z$) mixed with rare gases are commonly used for etching crystalline silicon and silicon oxide [4].

1.2.3Astrophysics

Electron-impact process also plays a major role in astrophysics. One example for this process is planetary nebulae. In the transition region of planetary nebulae, the free electrons are mixed with the neutral atoms such as H, He, C, N and O at moderately high temperatures. As a result, several formations and dissociations occur in this region and therefore significant amount of simple molecules like H_2, H_2^+, HeH^+, OH and CH^+ exist in the transition zones of nebulae. Since these formations or dissociations determine the availability of molecules and properties of the medium, electron impact cross sections are useful in the understanding of these kinetics behind planetary nebulaes [1].

Comet is another application where cross section information is commonly used in the field of astrophysics. C_2, CN, CH, NH, OH, CO, N_2, H_2 and their positive ions

have been recognized as primary constituents of a comet. Several ionization and excitation processes occur in comets due to solar wind electrons in the outer layer of the comet and photo electrons closer to the comet nucleus. These processes determine the kinetics of the comets and therefore accurate electron scattering cross sections are helpful in understanding the actual cometary processes [1].

1.2.4 Chemistry and Biological Science

Electron scattering cross sections are also important in radiation chemistry to diagnose the depth of the radiation damages in chemical systems. Scattering cross sections of hydrocarbon molecules are very useful in this field because most of the chemical systems are made out of hydrocarbon compounds. In related developments several authors have stressed the importance of electron scattering cross sections to develop models describing radiation damages to chemical systems like plastics and resins [5]. Radiation damages are also common for the living systems and it has been shown that DNA of living systems breaks due to ionization radiations. This occurs primarily due to collisions with free secondary electrons which are attached to the components of DNA molecules or to the water around them. Therefore collisions of electrons with atoms or molecules cause certain changes in living systems. Electron scattering cross sections are useful in the understanding of these processes and reducing the damage [6].

Mixed radioactive chemical wastes containing mixtures of wide variety of oxide materials, aqueous solvents and organic components are stored in underground storage tanks. These mixtures are continuously bombarded with energetic particles which are resulting from the decay of radioactive ^{137}Cs and ^{90}Sr. The highly energetic particles produced by these decays, lose their energy by interacting with atomic targets. As a

result of this energy loss process number of secondary electrons is produced. The collisions of these secondary electrons determine the chemistry of how these materials behave, and interact with the natural environment. So it is very important to understand electron interaction with the molecules present in these radioactive waste storage tanks because these processes can produce mixtures of toxic flammable and explosive gasses [4].

1.2.5 Liquid Phase Cross Sections

There are only very few cross section data available for condensed phase atoms or molecules. One major way of obtaining condensed phase cross sections is that deriving it using accurate sets of experimental and theoretical cross sections which are available for gas phase processes. So it is very important of having an accurate set of experimental cross section values for gas phase hydrocarbons to estimate the cross sections for liquid phase hydrocarbons [5].

1.3 Past Works

1.3.1 Experimental Studies

The electron collisions with atoms and molecules have been studied for almost a century, after the pioneering work of Frank and Hertz, and Ramseur [1]. The total electron scattering on hydrocarbons was first investigated by Brode [7], Bruche [8], Ramsauer and Kollath [9]. There after numerous experimental studies on electron scattering cross sections of hydrocarbons have been carried out.

From the beginning several experimental studies have been performed for total scattering cross sections of methane molecule. Hasted *et al*.[10] reported the TCS for CH_4 and C_2H_4 molecules. They have used the linear transmission method to measure the cross sections for the energies in between 0.3 and 5.0 electron Volts. Total electron scattering cross section for CH_4 also measured by Barbarito [11] for the energy range 0.05 to 6.0 eV using time of flight method (transmission method with time of flight discrimination). In 1985, Floeder and coworkers [12] measured the total scattering cross sections for a set of hydrocarbons namely, methane, ethane, propane, propene, cyclopropane, *n*-butane, isobutane and 1-butene. They also have used linear transmission technique to measure the TCS of these molecules in the energy range 100 - 400 eV. O. Sueoka and S. Mori [13] obtained the measurements for the total electron scattering cross sections of hydrocarbons for low and intermediate energies (0.7 – 400 eV). For their study, they have used retarding potential time of flight method (RP-TOF) to measure TCS of CH_4, C_2H_4 and C_2H_6. Total scattering cross sections of C_2H_4, C_2H_6, C_3H_6 (propene and cyclopropane) and C_3H_8 for the energies in between 4 – 500 eV have been reported by Nishimura and Tawara [14] and they have used a linear type electron transmission apparatus to obtain these measurements.

There were plenty of studies in the literature which present the total electron scattering cross section for methane molecule. But all these TCS values were limited to lower energies. In 1991 Zecca *et al*. [15] presented the total scattering cross sections for CH_4 for a wide energy range varying from 1 eV to 4000 eV. Later in 1998 Garcia and Monero [16] reported total scattering cross sections for CH_4 for the energies ranging from 400 eV to 5000 eV which obtained using linear transmission technique. Experimental

errors are estimated to be approximately 3% for this study. In Xing *et al*.[17] the absolute total scattering cross section measurements have been performed on the electron colliding with C_2H_2 molecule in the energy range 400 – 2600 eV. The linear transmission technique has used for this study and the estimated total experimental errors are about 5%. Tanaka *et al*.(1999) [18] presents the TCS measurements for C_3H_8 in the energy range 0.7 to 600 eV. They have used RP-TOF method to obtain these total electron scattering cross sections. An experimental study to measure the TCS of C_2H_6 and C_4H_{10} has been carried out by Sanches, Pinto and Iga [19] and they have measured TCS in the energy rage 100 eV to 1100 eV . In a previous experiment done at Baylor Van de Graaff laboratory, Ariyasinghe and Powers [20] measured TCS for the gases CH_4 ,C_2H_2, C_2H_4 and C_2H_6 in the energy range 200 – 1400 eV. TCSs for the electron scattering from two structured isomers of C_3H_6 (propene and cyclopropane) have been determined over the energy range from 0.5 up to 370 eV in a linear electron beam transmission experiment by Czeslaw Szmytkowski and Stanislaw Kwitnewski [21]. In 2002, they also reported [22] TCS s for some C_3 hydrocarbons namely C_3H_4 (Allene and Propyne), C_3H_6 and C_3H_8 for the same energy range. Total scattering cross sections by electron collisions with C_4H_6 and its isomers (1,3-butadiene and 2-butyne) have been measured by same experimental group in 2003, for the same energy range using the linear transmission technique[23]. In 2004, Thaminda Wijerathne [24] presented total electron scattering cross sections for CH_4 molecule for higher energies from 400 to 4000 eV. Results of this work have compared with other experimental studies and they are in good agreement with those of Garcia and Manero [16] for the entire energy range.

From above discussion it is clear that several experimental studies have been carried out to measure the TCS s of methane molecule. As a result there are plenty of TCSs available for CH_4 for the energy range 1 to 4000 eV. However the total cross section measurements in the intermediate and higher energies are scarce for the alkanes represented by $C_nH_{2(n+1)}$ (where n=2,3,4). The experimental total electron scattering cross section of ethane molecule (C_2H_6) is available for the energy range 0.7 to 1400 eV. There are no experimental TCS values reported for C_3H_8 molecule for the energies above 600 eV. For C_4H_{10} molecule, the experimental TCS values are reported only for the energy range 200 -1100 eV. For molecules C_4H_8 and C_4H_6, experimental TCS are reported, respectively, for energy ranges 200 – 1100 eV and 0.7 – 370 eV.

1.3.2 Theoretical Approaches

A few number of theoretical models have also been performed to predict the cross sections of hydrocarbons. There are three main theoretical approaches to predict the scattering cross sections namely Bethe-Born approximation, the spherical complex optical potential method (SCOP) and the additivity rule method. M. Inokuti [25] expressed the following theoretical model for cross section according to Bethe Born theory.

$$\frac{E}{R}\frac{\sigma}{\pi a_0^2} = A_{el} + B_{el}\frac{R}{E} + C_{el}\left[\frac{R}{E}\right]^2 + 4M_{tot}^2 \ln\left[2C_{tot}\frac{E}{R}\right] \qquad (1.1)$$

where E is the incident energy of electrons in eV, R is the Rydberg energy, a_0 is the Bohr radius and $A_{el}, B_{el}, C_{el}, M_{tot}$ *and* C_{tot} are constants which can be determined by the physical properties of the target gas.

Joshipura and Vinodkumar introduced the additivity rule and deduce formulas for cross section [26]. They proposed a formula for the total scattering cross section Q_T which is defined by,

$$\frac{Q_T}{a_0^{\,2}} = A\left(\frac{E_i}{keV}\right)^{-B} \tag{1.2}$$

Where a_0 is Bohr radius, E_i is the energy in keV, A, *B* are constants which can be determined by the molecular properties of the target gas. Referring this formula Garcia and Monero [27] proposed an empirical model for the cross section in terms of some molecular parameters for intermediate and high energies. According to their work,

$$\frac{Q_T}{a_0^2} = \left(0.4Z + 0.1\frac{\alpha_0}{a_0^2} + 0.7\right)\left(\frac{E}{keV}\right)^{-0.78} \tag{1.3}$$

where Z is the number of electrons in the target molecule and α_0 is the polarizability of the target molecule. All other parameters are having same meanings as in Joshipura's model. According to Garcia and Monero [27] this formula is valid only for molecules with 10< Z< 22.

Jiang, Sun and Wan [28] reported theoretical formula to calculate total electron scattering cross section by polyatomic molecules using additivity rule. First they defined TCS (elastic and inelastic) $Q_T(E)$ of the molecules using additivity rule and optical theorem as,

$$Q_T(E) = \sum_{j=1}^{N} q_T^j(E) \tag{1.4}$$

where, $q_T^j(E)$ is TCS due to the j^{th} atom of the molecule. Here $q_T^j(E)$,

$$q_T^j(E) = \frac{\pi}{k^2}\sum_{l=0}^{l_{\max}}(2l+1)\left[\left|1-S_i^j\right|^2 + \left(1-\left|S_i^j\right|^2\right)\right] \quad (1.5)$$

Where S_i^j is the l th complex scattering matrix element of the j th atom. S_i^j can be obtained by solving the radial equation with the optical potential V_{opt}, given by

$$V_{opt}(r) = V_s(r) + V_e(r) + V_p(r) + iV_a(r) \quad (1.6)$$

Here, $V_s(r), V_e(r), V_p(r)$ and $V_a(r)$ are respectively, static potential, exchange potential, polarization potential and absorption potential. This additivity rule has been modified considering the geometric shielding effect of molecules in 1997 by Jiang, Sun and Wan [29]. In their approach they have presented the total scattering cross section Q_{MT} as,

$$Q_{MT} = Q_{MG}(E) + A(Q_{MA}(E) - Q_{MG}(E)) \quad (1.7)$$

Where, $$Q_{MG}(E) = \frac{1}{3}Q_{//}(E) + \frac{2}{3}Q_{\perp}(E) \quad (1.8)$$

Here $Q_{//}$ and $Q_{\perp}$ are the TCS, respectively for the electron approaching the molecule parallel and perpendicular to the Z axis, while Q_{MA} is the $Q_T(E)$ given in equation (1.4).

The constant *A* is given by, $A = \frac{k^2}{mnC + k^2}$ and $k^2 = 2E$ and *E* is the energy of the incident electrons in units of eV, with *C = 1*. The *m* and *n* are the number of electrons and the number of atoms in the molecule, respectively. Later this formula has been modified for the shielding and overlapping effects by Sun *et al.* [30]. According to this study the TCS (Q_{MT}) of hydrocarbons can be written as,

$$Q_{MT} = \frac{1}{3}\sum_{j=1}^{m}\overline{C}_j q_T^j + \frac{2}{3}\sum_{j=1}^{n}\overline{C}_j q_T^j \quad (1.9)$$

q_T^j can be determined using equation (1.5) and $\overline{C}_j$ is a function of r_1 , r_2 (radii of two atoms) and d (bond length of two atoms). The two integers, m and n are the total number of atoms included to the $Q_{//}$ and $Q_{\perp}$ molecule units.

In the literature several authors [31,32,33] have used SCOP method and calculated cross sections for the molecules. Recently Vinodkumar *et al*.[34] calculated the Electron impact total (50 to 2000 eV) and ionization (threshold to 2000 eV) cross-sections for the hydrocarbon molecules CH_4,C_2H_2,C_2H_4,C_2H_6,C_3H_4,C_3H_6 and C_3H_8 and radicals CH_x (x=1,2,3) using SCOP and CSP-ic (Complex scattering potential-ionization contribution) Methods.

Other than these theoretical approaches there are some simple empirical formulas for TCS developed by analyzing the experimental cross section values. Floeder *et al*. [12] described the measured electron scattering cross sections by a simple formula containing the energy (*E*), number of electrons in the molecule (N_e) and three fitting parameters which were determined from their experimental cross sections. This empirical formula expresses the cross section $\sigma(E)$ as,

$$\sigma(E) = aN_e E^{-1/2}[1 + b\exp(-cE)] \tag{1.10}$$

where a, b, and c are the fitting parameters with numerical values respectively, $7.2\times10^{-16} cm^2 eV^{1/2}$, 0.17 *and* $(333eV)^{-1}$. They also have shown that the cross sections generated by this formula agree with their experimentally measured values for several hydrocarbons including methane, ethane, propane, butane and 1- butene in the energy range 100 - 400 eV.

In 1991 Nishimura and Tawara [14] presented a simple formula to determine the cross sections for intermediate energies based on the formula reported by Vogt and

Wannier (1954). According to Nishimura and Tawara [14], the total scattering cross section σ_T can be presented as,

$$\sigma_T = b/\sqrt{E} \tag{1.11}$$

Where, *b* is a constant for particular molecule and E is the energy of the electron. They have used this formula to calculate TCS of hydrocarbon molecules such as CH_4, C_2H_2, C_2H_4, C_2H_6 and C_3H_8 in the energy range 4 – 500 eV. In their study the constant b is given for these five molecules, so that the cross sections which can be obtained using this formula are limited to these molecules.

1.4 Present Study

The objective of this experiment is to measure the total scattering cross sections of some hydrocarbons, namely, C_2H_6 (Ethane), C_3H_8 (Propane), C_4H_{10} (n-Butane), C_4H_6 (1,3-Butadiene), & C_4H_8 (Butylene) for intermediate and high energies (300 eV – 4000 eV) using the linear transmission technique. The results of this experiment will be compared with the available experimental cross sections as well as the predictions of those by the theoretical models. This study will complete the available data for total electron scattering cross section for alkanes represent by $C_nH_{2(n+1)}$ where n=1,2,3,4 for the energy upto 4000 eV.

At the end a simple empirical formula will be developed to predict the cross sections of hydrocarbons by analyzing the present and existing experimental cross sections of hydrocarbon molecules. Though several experimental groups have proposed different empirical formulas, there exist considerable limitations of those in the determination of cross sections of larger hydrocarbon molecules. To overcome these

limitations present empirical formula will be developed based on the cross section per hydrogen atom and cross section per carbon atom.

CHAPTER TWO

Experimental Procedure

2.1 Determination of the Cross Sections

Linear transmission technique has been a popular method in the determination of electron scattering cross section because this method encounters minimum problems compared to other techniques [1]. In the present study the total electron scattering cross sections were measured using linear transmission technique. In this technique the attenuation of an electron beam passing through the target gas cell is measured. If the intensity of the electron beam which enters to the gas cell is I_0 and the intensity of the attenuated beam is I, the quantity I/I_0 can be related to the total scattering cross section by the well known Lambert- Beer law given by

$$\frac{I}{I_0} = \exp(-nPL\sigma_T) \tag{2.1}$$

where n is the number density of the target gas per unit pressure, P is the pressure of the gas, L is the scattering length of the cell and σ_T is the total electron scattering cross section. Both I and I_0 measurements can be obtained using a suitable monoenergetic electron current measuring device. The pressure of the gas cell can be measured by a manometer connected to the gas cell. After measuring I at different gas pressures (P) for a given I_0 at a certain electron energy and evaluating the slope of the plot $Ln(I/I_0)$ *vs* P, the total electron scattering cross section can be determined.

2.2 Experimental Arrangement

Given in Figure 2.1 is the schematic diagram for the experimental arrangement which was used to measure the total electron scattering cross sections for the present study. A Kimbal Physics EGG-3101 electron gun or the EFG-7 electron gun is used to produce a beam of electrons with energy between 300 - 4500 eV. Electron gun is mounted in a vacuum chamber which maintains very low (~ 10^{-7} *Torr*) pressure. This pressure is maintained inside the chamber using a set of turbo molecular and backing pump systems. The gas pressure at the electron gun position can be monitored by an ion gauge connected to the beam transport line. This electron beam passes through three well aligned apertures to produce a well collimated narrow electron beam. Then, this well collimated narrow electron beam enter the gas cell through entrance aperture. The length of the gas cell is variable and is defined by two aperture plates placed at entrance and exit of the gas cell. The pressure inside the gas cell was measured using a capacitance manometer connected to the gas cell. The target gas can be filled to the gas cell through gas inlet, by connecting an external gas cylinder to the inlet. The electrons exit from gas cell then enter to the Electro Static Analyzer (ESA) and the faraday cup combination which is mounted inside a vacuum chamber. ESA deflects inelastically scattered electrons and passes through the remaining pre selected mono energetic electrons. A Faraday cup is mounted at the exit aperture of the ESA and it detects the electrons emerging from ESA. The current generated at Faraday cup can be measured using an electrometer or a picoammeter. Another ion gauge is connected to the scattering chamber to monitor the pressure inside the chamber, where the ESA and faraday cup combination is housed.

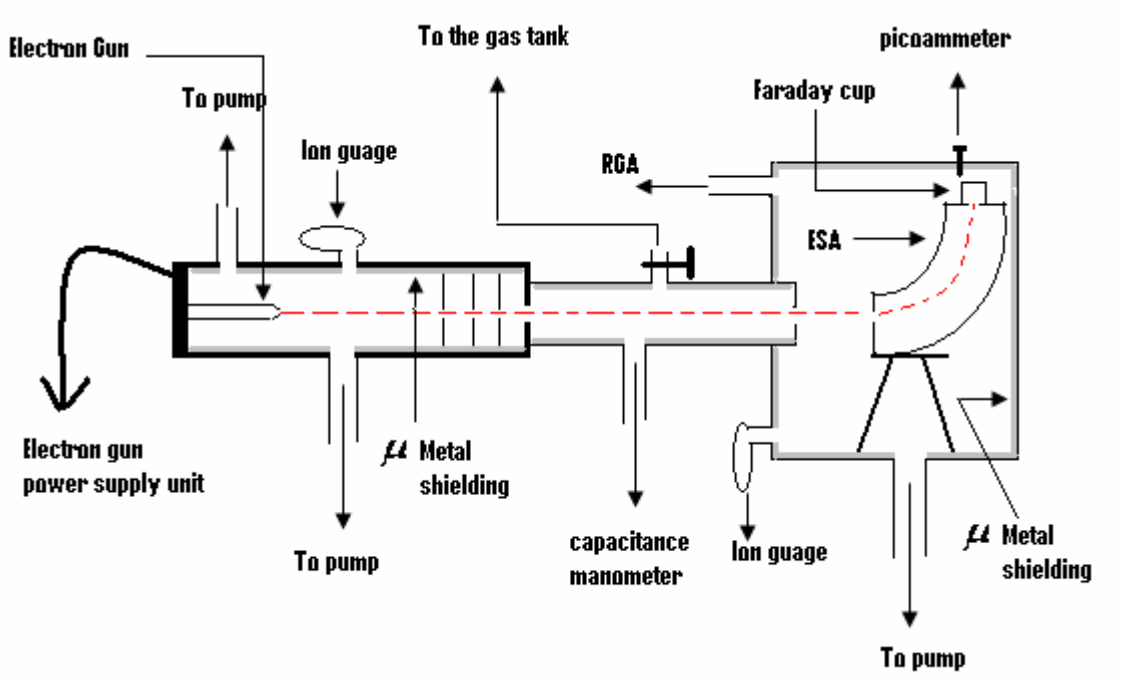

FIG.2.1.The schematic diagram for the experimental arrangement.

The entire setup including electron gun, gas cell, chamber with ESA and Faraday cup were kept in a vacuum of 10^{-7} *Torr* or better using turbomolecular pumps as well as a backing (rough) pumps. A layer of μ metal was used to shield the entire system from Earth's and other stray magnetic fields. A Residual Gas Analyzer (RGA) mounted in this chamber was used to guarantee the purity of the target gas inside the gas cell. Detailed information about each of these apparatus has been reported in the previous studies [20, 24, 35] which carried out in this laboratory. Therefore only a brief introduction for these apparatus will be included in the next seven sections.

2.2.1 Electron Gun and Power Supply Unit

The Kimball Physics EGG-3101 electron gun and the EFG-7 electron gun were used to produce the high energy and low energy electron beams respectively. The Kimball EFG-7 electron gun provides a uniform wide angle low energy electron beam.

This was used to produce an electron beam with energy 300 eV to 1000 eV. The Kimball physics EGG-3101 electron gun was used to produce a well collimated, low current small spot, high energy electron beam. In this electron gun, beam current and beam energy are adjustable over wide ranges and the energy can be varied from 1 keV to 10 keV [36]. This gun has been used for the present work to produce an electron beam with energy ranging from 1000 eV to 4500 eV.

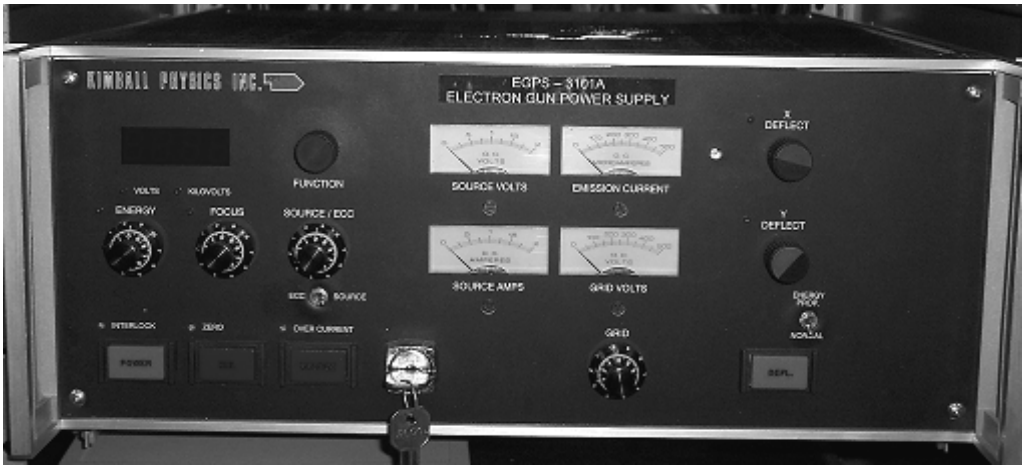

FIG.2.2. EGPS 3101 electron gun control unit.

EGPS-3101 and EFPS-7 electron gun control units were used to generate the necessary voltages to run the two electron guns Kimball Physics EGG-3101 and EFG-7 respectively. These control units have the capability of changing the focusing of beam and deflecting it horizontally or vertically. The electron gun is also equipped with a triode to produce and control the electron beam. Triode consists of three elements namely cathode, Wehnelt (Grid) and grounded anode. Electrons emitted from the cathode are accelerated by the triode's electric field. This causes the beam to crossover in the triode region. This crossover forms an object to the focusing lens which produces an

image at the target [37]. The energy and the path of the electrons are determined by the magnitude and the direction of the electric field created due to the potential difference between the cathode and anode. When the grid potential is varied, the electric field between the cathode and the grid changes the electron emission from the cathode. Therefore the grid potential can be utilized as an emission current control.

2.2.2 Gas Cell and Gas Delivery System

Given in Figure 2.3 is the cross sectional view of the gas cell where the electron scattering take place. The gas cell is made out of Aluminum. Length of the gas cell is set to 24.5 cm which is defined by entrance and the exit apertures with diameters 0.75 mm and 1mm respectively.

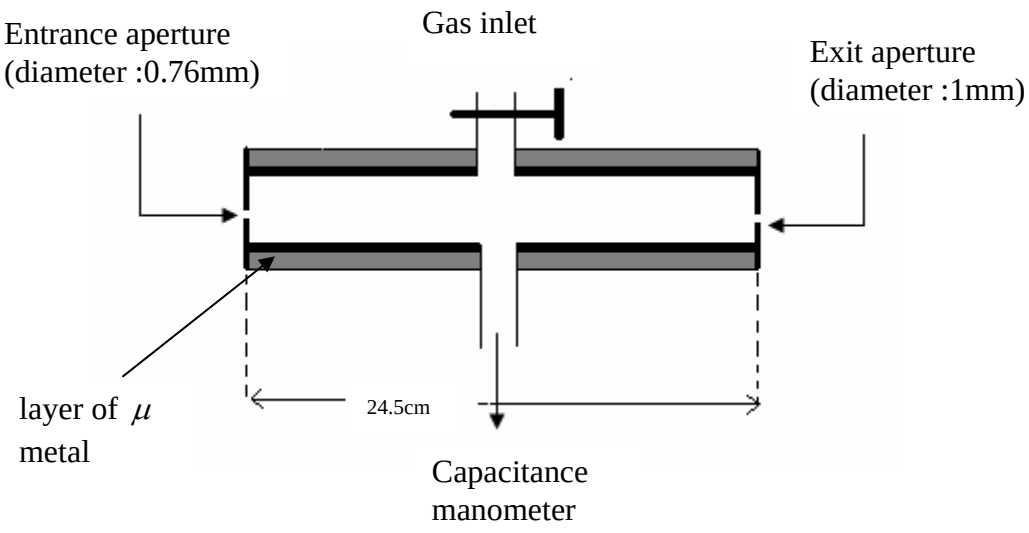

FIG.2.3. The cross sectional view of the gas cell.

A layer of μ metal is there in the gas cell, to shield the electron beam from earth's and other stray magnetic fields. Pressure inside the gas cell was measured using capacitance manometer connected to the gas cell. Gas inlet was used to send the target gas to the gas

cell from externally connected cylinder. The gas flow from the gas cylinder to the gas cell was controlled by a regulator, course needle valve and fine needle valve.

FIG.2.4 : The externally connected gas cylinder with the regulator.

Table 2.1 .The purities of gases

Gas	Purity
Ethane	99.9%
Propane	99.9%
Butane	99.9%
1,3 Butadiene	99.5%
Butylene	99.0%

Gas cylinder contains the appropriate target gas used for the experiment and these were commercially purchased from Methason Gas products and Praxair Inc. . The purity

of these gases were 99.0% or better. Given in Table 2.1 are the purities of the gases as claimed by the manufacturers.

2.2.3 Capacitance Manometer

MKS Baratron 626 A capacitance manometer was used to measure the pressure inside the target gas cell. This pressure transducer system converts the pressure to a linear dc voltage output using a sensor, signal conditioner and a power supply. The sensor in this capacitance manometer consists of a pressure inlet tube which is connected to a small chamber in the transducer. One wall of this chamber is an elastic metal diaphragm. Front side of this diaphragm is open to the gas, whose pressure is to be measured and the other side of the diaphragm faces to a ceramic disc with two electrodes. When the absolute pressure gets changed, the diaphragm turns aside regardless of the gas type. The distance to the diaphragm is now different for each electrode and this results an imbalance of the electrode capacitances. This imbalance of capacitance is converted to a dc voltage and sent through the signal conditioner to produce a precise signal [38]. This signal was read using MKR PDR-D readout display unit which could be use to read the pressure to 0.01 *mTorr.*

2.2.4 Electrostatic Analyzer

A Comstock model AC-901 double focusing electrostatic analyzer was used to detect elastically scattered electrons. The ESA is housed in a vacuum chamber as shown in Figure 2.5 which is made out of soft iron with an aluminum base plate. A certain voltage difference is applied between the spherical sectors of ESA, to keep the analyzer in a constant transmission mode, so that the electrons with predetermined constant energy

will only transmit through the ESA to the exit aperture. A retarding bias voltage was applied to the entrance aperture plate of the ESA to deflect away the low energy electrons at the entrance and to reduce the kinetic energy of entering electrons to an energy equivalent to the pre-set transmission energy.

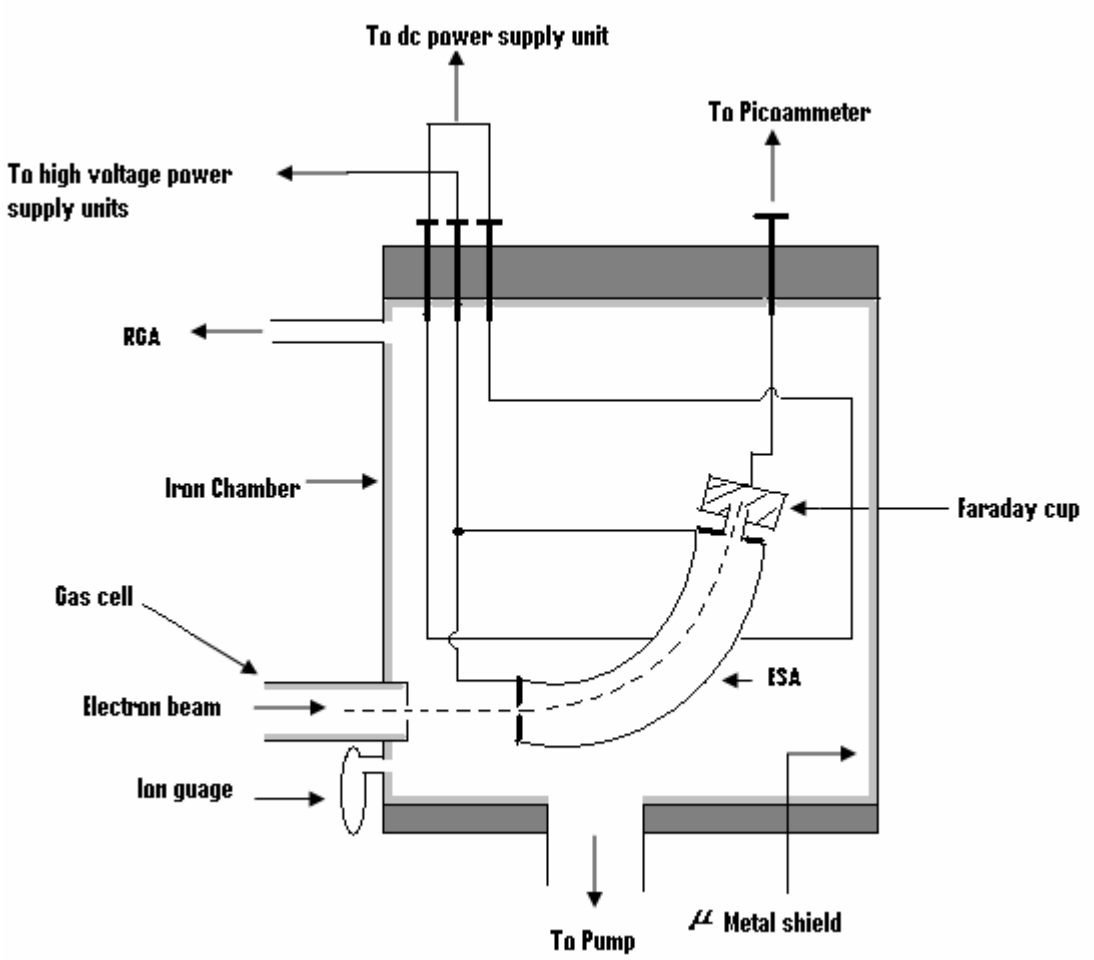

FIG.2.5. A cross sectional view of the chamber containing ESA

In the present study, two transmission energies were used depending on the energy of the incident electrons. 100 eV constant transmission energy was used for the electrons with energy 300 eV to 2000 eV while 150 eV constant transmission energy was

used for the electrons with energy 2000 eV to 4500 eV. The two transmission energies 100 eV and 150 eV were obtained by applying 44.4V and 66.58V respectively across the spherical sectors of the ESA. This potential difference was given using Eveready, model NEDA 710, dc batteries. Series combination of two power supplies was used to apply the retarding bias voltage. BERTAN model 230-03 high power supplies were used for this purpose and each was capable of producing voltage 0-3000 V. When the energy of incident electrons is 1200 eV and if retarding voltage of -1100 V is applied to the entrance of the ESA and 44.4 V is applied across spherical sectors, the electrons will passes through the ESA with 100 eV transmission energy. These electrons will be collected by the Faraday cup placed at the exit aperture of the ESA.

2.2.5 Faraday Cup and Picoameter

Electrons transmitted through the ESA were collected using Faraday cup and measured by the electrometer. Faraday cup is cylindrical in shape with the diameter of 0.4 cm and 2 cm in height. The current generated at the faraday cup was measured by a Keithley model 480 picoammeter which is having accuracy of 0.01 pA. This is a $3\frac{1}{2}$ digit picoammeter that provides seven decade current ranges from 10^{-9} to 10^{-3} A. As given in Figure 2.6 the Keithley model 480 picoammeter includes a current to voltage converter, a $3\frac{1}{2}$ digit analog to digital converter and display and a power supply [39].

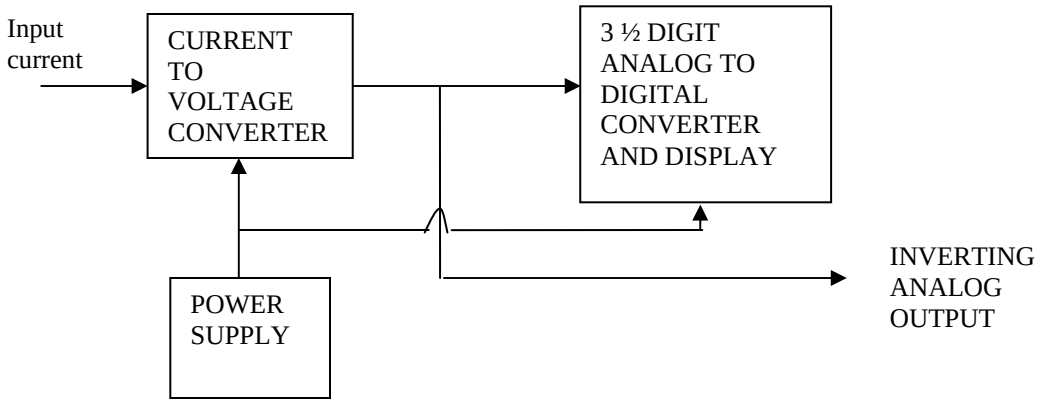

FIG.2.6. A schematic diagram of the circuitry of Keithley model 480 picoammeter [39]

2.2.6 Residual Gas Analyzer

The purity of gasses inside the scattering chamber was monitored using an Ametek Dycor model 1200 Quadrapole Gas Analyzer along with an Ametek MA100 analyzer head. This apparatus measures the partial pressures of the constituents of gasses inside the scattering chamber. In the analyzer head, electrons are produced from a hot filament and these electrons collide with the molecules in the ionization region of the analyzer head. This process results the ions of molecules as well as ion fragments. These ions are directed to a mass filter which accepts only the ions with specific mass-to-charge ratio. These mass filtered ions are then converted to an electric current which is proportional to the corresponding molecular partial pressures [40]. These pressure values were obtained by the Ametek Dycor model LC200 interface via computer . Given in Figure 2.7 is the graphical representation of the partial pressures as given in Dycor software.

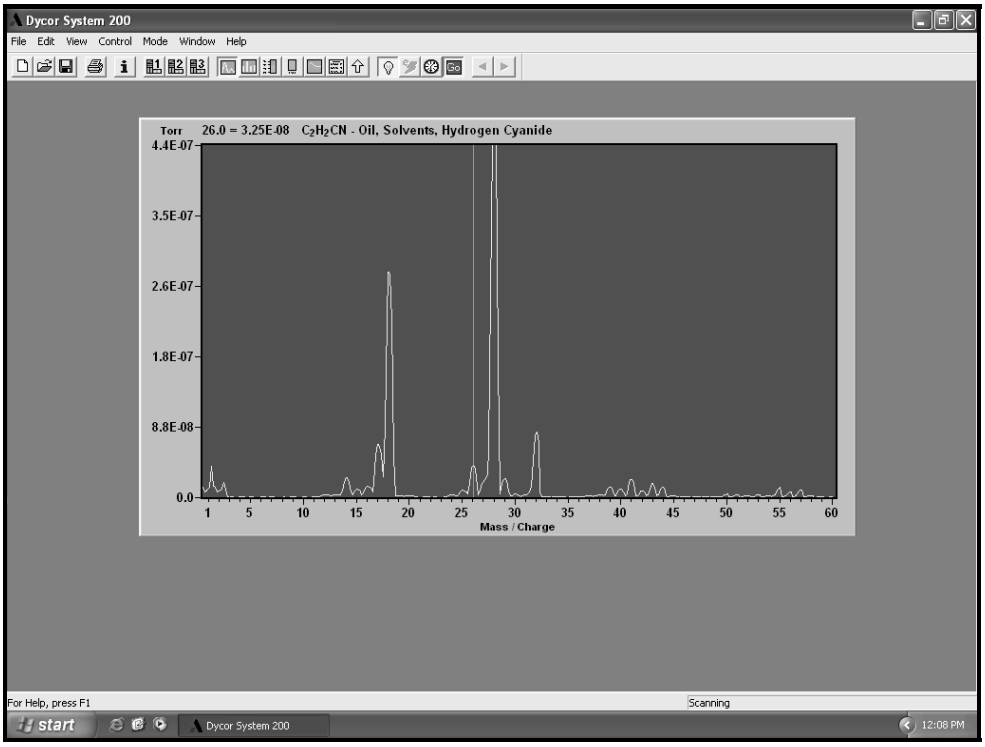

FIG.2.7. Graphics mode pressure scanning screen in Dycor LC200 interface.

2.2.7 Vacuum Systems and Shielding

Two sets of turbomolecular pumps and backing pumps were used to keep the entire set up in a vacuum. Since the target gasses used for the study are heavy hydrocarbons, there is a high possibility of fragment them to ions inside the gas cell. An additional turbomolecular pump was used at electron gun chamber to prevent the system from these ions and maintain the pressure at 10^{-7} *Torr* region. A 1.5 mm thick μ metal layer is in the entire path of the electron beam including the electron gun chamber, gas cell and the scattering chamber, to shield the electron beam from Earth's and other stray magnetic fields.

2.3 Experimental Procedure

At first, the pressure inside the gas cell and the chamber area was checked with two ion gauges. If the pressure everywhere is in the range of 10^{-6} *Torr* region, the system is suitable to run the experiment. Generally the pressure value at ion gauge is 2.4×10^{-6} *Torr* . The small turbomolecular pump connected to the electron gun chamber is then turned on and the pressure inside the electron gun region and the gas cell is further reduced to lower 10^{-7} *Torr* range. The RGA was turned on and allowed to warm up for 15 - 20 minutes. The gas cell and the gas delivery lines were then purged using the target gas. In this purging procedure, gas cell and the delivery lines were first filled with the target gas and kept it for about 3 seconds. Then the external supply of the target gas was closed, so that the target gas inside the gas cell and delivery system were flushed out by pumps. These purging steps were carried out for about 5 to 6 times to reduce the environmental contaminants inside the system. Then the purity of gasses inside the system was monitored using RGA along with the Dycor interface through the computer.

In order to confirm the purity of the gasses and to justify that there is no air contamination during the transfer of gasses from gas cylinders to the gas cell following procedure was used. First the partial pressures of the background gasses were monitored and the partial pressures of oxygen (32) and the hydrocarbon target gases were recorded. Then the target gas was admitted to the gas cell through the gas inlet and the changes in the partial pressures were monitored. The new pressures of the oxygen and the target gas were recorded after admitting the gas to the cell. If the partial pressure level of oxygen had gone down, that verifies 99% or higher percentage of the target gas is inside the gas cell. Normally the recorded background partial pressures for hydrocarbon target gas and

for Oxygen (32) were respectively, in the orders of 10^{-9} and 10^{-8} *Torr* regions and the total pressure of the gas cell was in the order of 10^{-7} *Torr* region. After the admittance of target gas to the cell, the partial pressure of the target gas was increased to the order of 10^{-6} *Torr* region while the total pressure inside the gas cell was also in 10^{-6} *Torr* region. The partial pressure of Oxygen was decreased within the 10^{-8} *Torr* region, while the partial pressure of target gas increased by a factor of 100 or more. Therefore new partial pressure of Oxygen is 1% or less compared to the total pressure of the cell and this confirms that the purity of the target gas inside the gas cell should be 99% or better. The partial pressure of Oxygen went down because the total pressure inside the cell was increased and this reduces the out gassing of gases (including O_2) to the cell from its walls. In the previous studies, the partial pressure of nitrogen has been used to verify the purity in most cases. nitrogen cannot use for this study because inside RGA there is a possibility to create hydrocarbon fragments with mass number 28 (for an example C_2H_4) which is equal to nitrogen's.

The digital readout for the MKS capacitance manometer was then checked and zeroed if it is not zero at the beginning. Next the voltage across the two hemispherical plates of ESA was set to the appropriate voltage depending on the transmission energy and this voltage was further checked using a digital multimeter. For the present study two voltages 44.4 V and 66.6V were used to obtain transmission energies of 100 eV and 150 eV respectively. The retarding bias voltage was then set according to the energy of the electron beam. For an example, to obtain the attenuation current for electrons with 1200 eV, retarding bias voltage is set to 1100 V. The retarding bias voltage here is 100 V less than the electron energy, since the transmission energy for this case is 100eV.

After all mentioned pre preparations, the electron gun was turned on. The electron emission current was set to about $10\mu A$ and the electron energy was set accordingly at the electron gun power supply unit. The electron gun was then kept for at least 30 minutes until the electron gun filament is warmed up. If the filament is warmed up, the picoammeter reading becomes stable in a certain value. Next, the current of the faraday cup or the picoammeter reading was maximized by adjusting the electron energy. In this procedure the electron energy is selected to match the preset energies in the ESA to the nearest 0.1 eV. Then the gun emission current is adjusted to 100 pA either by the grid voltage or the source voltage. This current is the intensity of the electron beam enters to the gas cell (I_0), in equation 2.1. Gas was then allowed to enter to the gas cell by opening the gas inlet valve. At this moment the pressure shown at the capacitance manometer was recorded along with the intensity of the attenuated beam measured by picoammeter. The gas cell inlet valve is then closed and allow the pressure of the system to be settle at initial value which was about $2.4\times10^{-7}Torr$, before going to the next measurement. The attenuated currents for eight different pressure values were obtained per each energy by repeating this procedure. Then to study the next energy, the retarding bias voltage was set accordingly as previously mentioned. Electron beam energy is then changed to the new energy and obtained the appropriate intensities of the attenuated beam along with the pressure values, by repeating the same procedure. Six sets of measurements were taken for each energy ranging from 300 – 4500 eV with certain energy gaps.

The temperature inside the gas cell is required to calculate the number density of the target gas inside the gas cell. In previous studies [35, 41] it has been investigated that

there is no significant different in temperatures inside and immediate outside the gas cell. Therefore the temperature near the gas cell was recorded during the experiment and generally it was 20^{o}C and no considerable variations were observed.

2.4 Estimation of Errors

The total electron scattering cross sections determined using above mentioned procedure also contain certain unavoidable errors associated with them. These errors are due to six main sources, namely,(1) determination of gas-electron interaction length,(2) emission current variations,(3) fluctuations of attenuation current, (4) pressure measurement, (5) purity of gas inside the cell, and (6) the statistical error due to standard deviation. These errors which cause the uncertainties in determination of total scattering cross sections will be discussed in this section along with their percentage contribution to the total error.

In this study, the gas- electron interaction length (L) is an important measurement to determine the total scattering cross section. The error causes here because of effusion of gas molecules through exit and entrance apertures of the gas cell due to the pressure gradient between inside and outside the gas cell. The geometrical length of the gas cell was 24.5 cm for this study and a correction factor should be added to this in order to get accurate effective gas-electron interaction length. Evaluation of this factor for the gas cells with different lengths has been carried out in a previous study [42] performed in this laboratory. According to that, the estimated error of length due to gas effusion is about 3 mm for each side for the gas cell used for present study. Therefore the total percentage error of gas electron interaction length is $\pm 2.5\%$.

The initial emission current (I_0) of the electron beam is set to 100 pA when there is no target gas inside the cell. This emission current does not remain same with the presence of target gas. It was observed the changes are higher for the heavier hydrocarbons with double bonds (C==C) compared to linear alkanes. Considering this effect due to the change of emission current, an error of 3% was estimated for the hydrocarbons C_4H_8 and C_4H_6 and $\pm 2\%$ was estimated for the other hydrocarbons used for this study. Another error in the current measurement is cause due to fluctuations of current around 100 pA. In some cases the picoammeter reading will not reset exactly to 100 pA after one reading but it will fluctuate in between 99 and 101 pA. This effect contributes $\pm 1\%$ of error for the final total cross sections.

One other major cause of error is the systematic error of the capacitance manometer. An error occurs here because of approximations of values and this error is a constant value for all pressures, so that percentage error due to this varies depending on the pressure value. For an example manometer gives 4.0 *mTorr* for the values from 3.99 to 4.01 *mTorr* and 2.0 *mTorr* for the values ranging from 1.99 *mTorr* to 2.01 *mTorr etc.*. An error of ± 0.01 *mTorr* occurs for all pressure values and the percentage error due to this is therefore varies from 4% to 0% for the pressure values from 0 to 4.0 *mTorr*. Therefore an average error of $\pm 2\%$ was added as the error of pressure measurement, considering the range of pressure values from 0 to 4.0 *mTorr* used for the present study.

The purity of the gas inside the gas cell was monitored and confirmed to that 99% of target gas is there inside the cell. But still there is a 1% or less percentage of error which is unavoidable. The slopes of the plots of $\ln\left(I/I_0\right)$ vs P were evaluated using

least square method and there is a $\pm 1\%$ or less percentage of statistical error due to standard deviation.

The total error for the total cross section was calculated considering error of electron gas interaction length which is $\pm 2.5\%$, error of current fluctuations which are $\pm 2\%$ or $\pm 3\%$ (for C_4H_8 and C_4H_6) and $\pm 1\%$, the error associated with pressure measurement which is $\pm 2\%$, error of gas purity which is $\pm 1\%$ and $\pm 1\%$ statistical error of standard deviations. According to these facts the error for the total scattering cross section was estimated by adding them in quadratures, and it is $\pm 4\%$ for the molecules C_2H_6, C_3H_8, C_4H_{10} and $\pm 5\%$ for the C_4H_8 and C_4H_6.

CHAPTER THREE

Results and Analysis

3.1 Experimental Results and Analysis

3.1.1 Determination of Experimental Scattering Cross Sections

The attenuation current (I) along with the appropriate pressure (P) was measured for each energy, using the procedure explained in chapter two. Then the slopes of linear regression lines of plots $\ln(I/I_0)$ vs P were obtained for all experimental trials carried out for each energy. Figure 3.1 represents the variation of $\ln(I/I_0)$ vs P and the respective regression lines for the target gas C_4H_6 for the selected energies between 300 eV to 4000 eV. The variations of $\ln(I/I_0)$ with *P* for the other gasses are identical to the Figure 3.1 with the exception of different slopes. The regression lines were obtained using the least square method. The total electron scattering cross sections for the target gasses were obtained using the following equation, which is derived from the Lambert Beer Law (Eq. 2.1) and the universal gas law.

$$\sigma_T = \left(\frac{1}{nL}\right)|Slope| \tag{3.1}$$

where *n* is the number density of the gas at a unit pressure, *L* is the scattering length of the gas cell. Slope is the gradient of the regression lines obtained for plots $\ln(I/I_0)$ vs P. The total electron scattering cross sections for the target gasses were determined by using respective slopes to equation (3.1). The measured cross sections for linear alkanes C_2H_6, C_3H_8 and C_4H_{10} are given in Table 3.1 with the error associated with it. Given in

Table 3.2 are the total electron scattering cross sections obtained for C_4H_6 and C_4H_8 molecules.

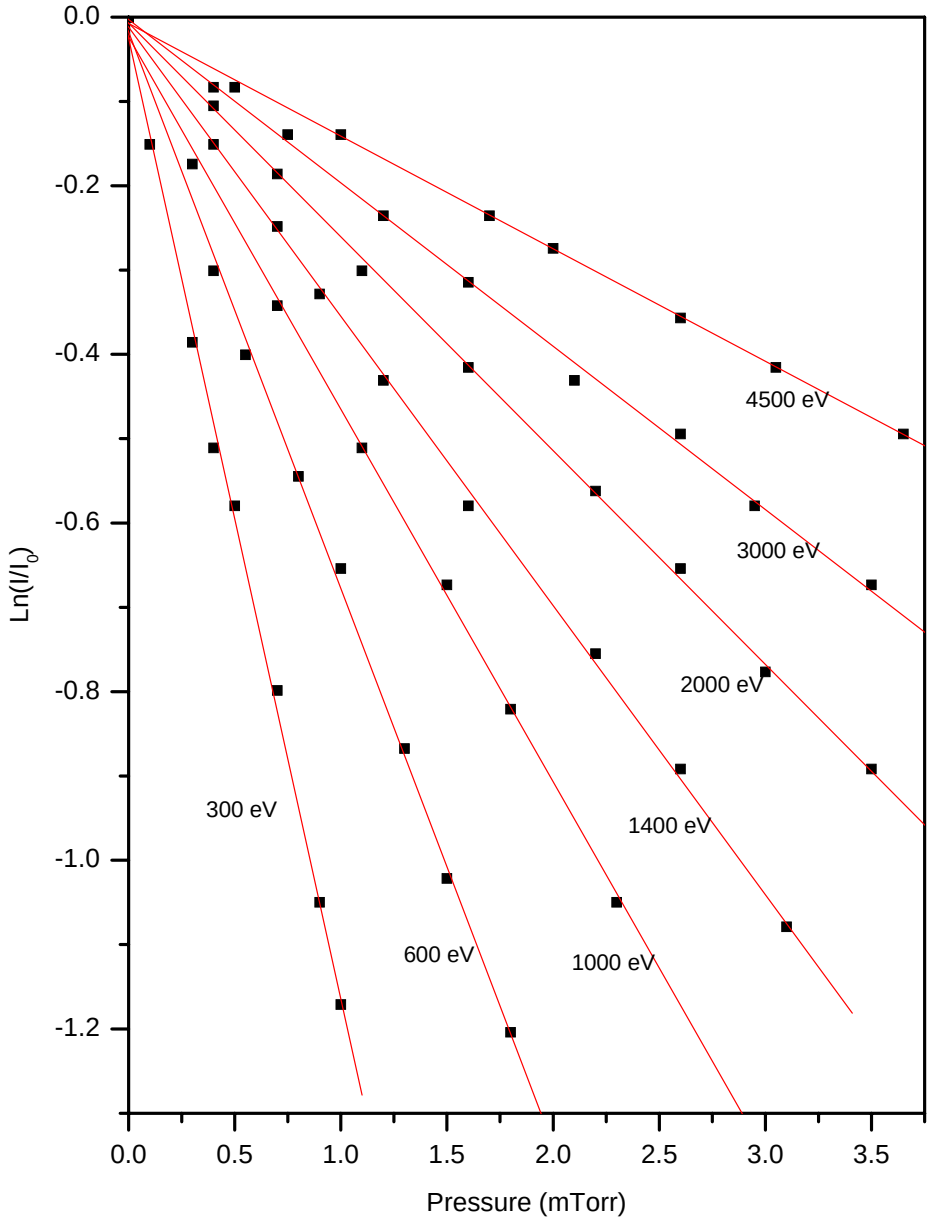

FIG 3.1. Variation of $\ln\left(I/I_0\right)$ with pressure for C_4H_6 at certain energies between 300 eV and 4000 eV.

Table 3.l. Measured total electron scattering cross sections for the molecules C_2H_6 , C_3H_8 and C_4H_{10} in the units of $10^{-20}\ m^2$.

Energy (eV)	C_2H_6	C_3H_8	C_4H_{10}
300	9.15 ± 0.37	11.98 ± 0.48	14.81 ± 0.59
400	7.53 ± 0.30	9.95 ± 0.40	12.31 ± 0.49
500	6.49 ± 0.26	8.62 ± 0.34	10.81 ± 0.43
600	5.33 ± 0.21	7.60 ± 0.30	9.15 ± 0.37
700	4.72 ± 0.19	6.62 ± 0.26	8.28 ± 0.33
800	4.30 ± 0.17	5.89 ± 0.24	7.63 ± 0.31
900		5.39 ± 0.22	6.90 ± 0.28
1000	3.47 ± 0.14	4.97 ± 0.20	6.36 ± 0.25
1100	3.28 ± 0.13	4.65 ± 0.19	6.11 ± 0.24
1200	3.07 ± 0.12	4.27 ± 0.17	5.60 ± 0.22
1300			5.12 ± 0.20
1400	2.67 ± 0.11	3.85 ± 0.15	4.83 ± 0.19
1600	2.41 ± 0.10	3.41 ± 0.14	4.21 ± 0.17
1800	2.22 ± 0.09	3.07 ± 0.12	3.90 ± 0.16
2000	2.01 ± 0.08	2.66 ± 0.11	3.50 ± 0.14
2250	1.77 ± 0.07	2.54 ± 0.10	3.08 ± 0.12
2500	1.61 ± 0.06	2.25 ± 0.09	2.91 ± 0.11
2750	1.53 ± 0.06	2.14 ± 0.09	2.80 ± 0.11
3000	1.37 ± 0.05	1.99 ± 0.08	2.57 ± 0.11
3500	1.23 ± 0.05	1.61 ± 0.06	2.26 ± 0.09
4000	1.10 ± 0.04	1.44 ± 0.06	2.01 ± 0.08

Table 3.2. Measured total scattering cross sections for the hydrocarbon molecules C_4H_6 and C_4H_8 in the units of $10^{-20}\ m^2$.

Energy (eV)	C_4H_8	C_4H_6
300	14.85 ± 0.74	14.12 ± 0.71
400	11.09 ± 0.55	10.43 ± 0.52
500	9.50 ± 0.47	8.95 ± 0.45
600	8.45 ± 0.42	7.99 ± 0.40
700	7.84 ± 0.39	7.21 ± 0.36
800	6.92 ± 0.35	6.59 ± 0.33
900	6.26 ± 0.31	5.88 ± 0.29
1000	5.71 ± 0.29	5.41 ± 0.27
1100	5.23 ± 0.26	5.19 ± 0.26
1200	5.03 ± 0.25	4.88 ± 0.24
1300	4.77 ± 0.24	4.52 ± 0.23
1400	4.43 ± 0.22	4.12 ± 0.21
1600	4.00 ± 0.20	3.73 ± 0.19
1800	4.03 ± 0.20	3.36 ± 0.17
2000	3.65 ± 0.18	3.19 ± 0.16
2250	3.23 ± 0.16	3.06 ± 0.15
2500	2.81 ± 0.14	2.69 ± 0.13
2750	2.62 ± 0.13	2.51 ± 0.13
3000	2.36 ± 0.12	2.37 ± 0.12
3500	2.19 ± 0.11	2.08 ± 0.10
4000	1.93 ± 0.10	1.79 ± 0.09
4500	1.79 ± 0.09	1.60 ± 0.08

3.1.2 Comparison with Other Experimental and Theoretical Results

As mentioned in Chapter two, the total electron scattering cross sections for hydrocarbon molecules have been studied by several authors for lower energy ranges. The scattering cross sections for intermediate and high energy range are not available in the literature for the heavier molecules like C_4H_{10}, C_4H_8 and C_4H_6. Therefore the results obtained from the present study for C_2H_6 and C_3H_8 were compared to the results of available experimental and theoretical cross sections. These comparisons of results with available experimental and theoretical studies will be discussed in next few sections.

3.1.2.1 Ethane (C_2H_6) There is one experimental study carried out for the total electron scattering cross sections of ethane molecule in an energy range overlapping with the energy range of the present experiment. Sueoka and Mori [13] measured the TCS for C_2H_6 at electron energies up to to 400 eV. Three groups, Garcia and Monero [27], Sun *et al*. [30] and Vinodkumar *et al.*[34], have predicted the TCS of C_2H_6 at energies higher than 300 eV using theoretical or empirical models. Garcia [27] proposed an empirical formula (Eq 1.3) to predict the cross sections in the energy range 0.5 - 5 keV for molecules whose number of electrons between 10 and 22. This can be used to compare the cross sections of ethane obtained from the present study since it is a molecule with 18 electrons. Sun *et al.* [30] proposed a theoretical formula to obtain the cross section of C_2H_6 up to 2000 eV electron energy. Recently, Vinodkumar *et al.* [34] reported a theoretical model to calculate total scattering cross sections of hydrocarbon molecules including C_2H_6 up to 2000 eV. Given in table 3.3 are the scattering cross sections for C_2H_6, obtained from present experimental study along with available experimental and theoretical cross sections in the literature over the range of energy from 100 – 4000 eV.

Table 3.3. The experimental and theoretical total electron scattering cross sections for C_2H_6 in the units of $10^{-20} m^2$.

	Experimental		Theoretical		
Energy (eV)	Present	Sueoka & Mori [13]	Sun *et al.* [30]	Garcia & Monero [27]	Vinodkumar *et al.* [34]
100		12.7	15.28		13.5
120		11.8	13.90		
150		10.5	12.34		11.4
200		9.2	10.46		9.87
250		8.2	9.08		
300	9.15	7.6	8.00		8.91
350		6.9	7.14		
400	7.54	6.2	6.43		7.06
500	6.49		5.32	5.24	6.21
600	5.33		4.49	4.54	5.52
700	4.72		3.85	4.03	5.02
800	4.30		3.35	3.63	4.52
900			2.94	3.31	4.11
1000	3.47		2.61	3.05	3.81
1100	3.28		2.34	2.83	
1200	3.07		2.13	2.65	
1300			1.98	2.49	
1400	2.67		1.86	2.35	
1500			1.80	2.22	2.67
1600	2.41		1.78	2.11	
1800	2.22		1.87	1.93	
2000	2.01		2.15	1.78	2.11
2250	1.77			1.62	
2500	1.61			1.49	
2750	1.53			1.39	
3000	1.37			1.29	
3500	1.24			1.15	
4000	1.10			1.03	

A graphical representation of these previously reported experimental and theoretical cross sections with those presently determined for C_2H_6 is included in Figure 3.2 for better comparison.

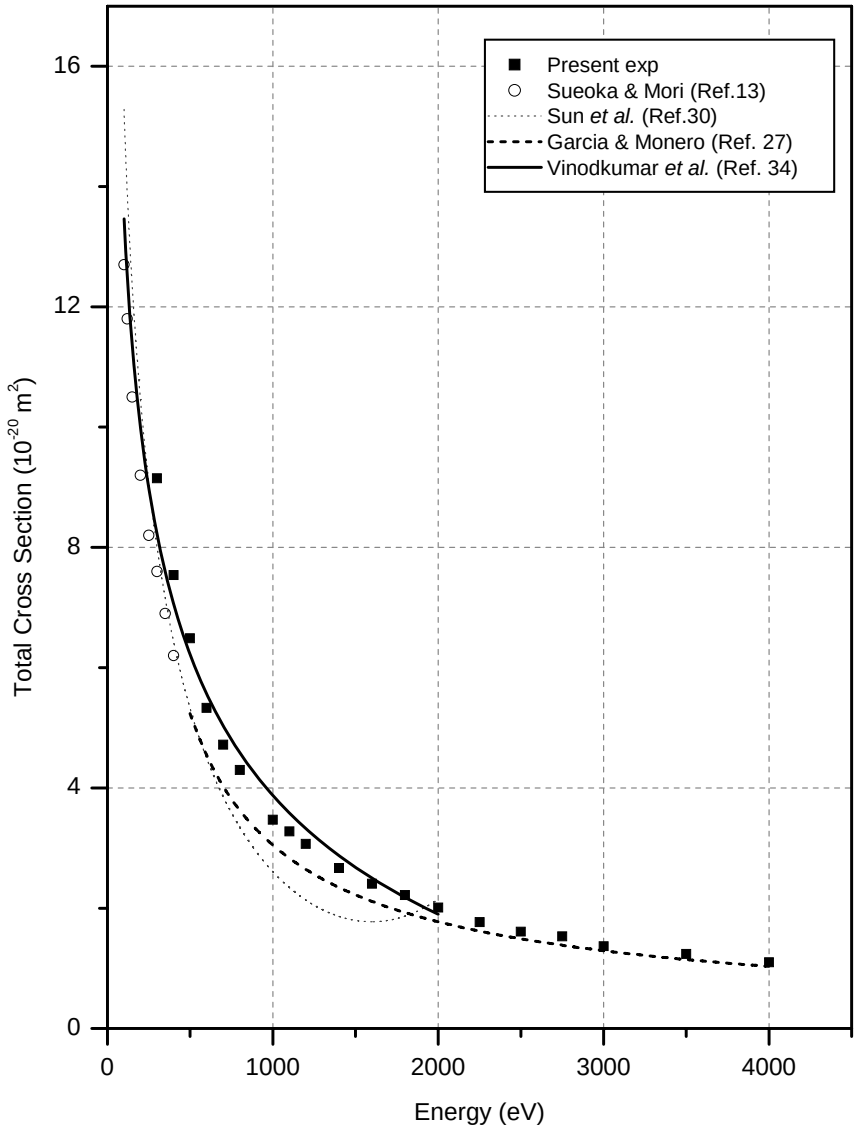

FIG 3.2. Total electron scattering cross sections for C_2H_6 in the units of $10^{-20}\,m^2$ for the energy range 100 to 4000 eV. Squares represent the experimental results of present work and circles represent the experimental cross sections of Sueoka & Mori [13]. Dotted and Solid lines are from Sun *et al.* [30] and Vinodkumar *et al.* [34] respectively. Dashed line represents the theoretical results obtained by Garcia and Monero [27].

As can be seen from Figure 3.2, the experimental cross sections obtained for C_2H_6 in this study are in closer agreement with the cross sections predicted by Vinodkumar [34] for the energy range 100 to 2000 eV. For the energies greater than 2000 eV, the theoretical

cross sections calculated by Garcia and Monero [27] are in agreement with the experimental cross sections of present study. However their model under predicts the TCS at energies below 2000 eV. The theoretical predictions by Sun and coworkers [30] are 0-30 % lower than the present experimental results for energies 300 – 1000 eV. In summary, the cross sections in Ref. 34 follow the general trend of the experimental cross sections while those in the Ref. 30, are highly deviated from the experimental cross sections of the present study. The cross sections produced in the present study at 300 eV and 400 eV energies are 10 – 18% higher than those of experimental cross sections of Sueoka and Mori [13]. According to my knowledge, there are no other experimental cross section measurements available among the past works to compare with the present cross sections of ethane.

3.1.2.2 Propane (C_3H_8) Experimental studies to evaluate the total scattering cross sections of propane have been carried out by few experimental groups. As mentioned in Chapter two Szmytkowski and Kwitnewski [21] reported experimental measurements for C_3H_8 for the low energies from 0.5 eV to 370 eV. The measurements reported in reference 21 and theoretical predictions by Sun *et al.* [30] and Vinodkumar *et al.* [34], along with the results of present study are given in Table 3.4. The graphical comparison of this study with previous studies is shown in Figure 3.3.

From the cross sections given in Table 3.4 and the Figure 3.3 it is clear that the experimental cross sections of the present study are in good agreement with those of Szmytkowski and Kwitnewski [21] for the energy range 100 – 370 eV. For C_3H_8, there are no experimental measurements available in the literature for energies greater than 370 eV for the comparison with the present measurements. The experimental measurements

Table 3.4. The experimental and theoretical total electron scattering cross sections for C_3H_8 in the units of $10^{-20} m^2$.

	Experimental		Theoretical	
Energy (eV)	Present	Ref. 21	Sun *et al.* [30]	Vinodkumar *et al.* [34]
100		24.0	25.57	15.9
110		23.1	24.35	
120		21.7	23.29	
140		20.2	21.49	
150			20.72	12.7
160		18.8	20.00	
180		18.0	18.72	
200		16.7	17.29	10.8
220		16.0	16.60	
250		14.2	15.30	
275		13.6	14.35	
300	11.98	12.6	13.32	8.72
350		11.3	12.07	
370		10.7	11.56	
400	9.95		10.74	7.43
500	8.62		8.91	6.55
600	7.60		7.54	5.86
700	6.62		6.48	5.49
800	5.89		5.63	5.1
900	5.39		4.95	4.78
1000	4.97		4.40	4.4
1100	4.65		3.62	
1200	4.28		3.14	
1300			3.34	
1400	3.85		3.14	
1500			3.02	3.43
1600	3.41		2.96	
1800	3.07		3.08	
2000	2.66		3.49	2.65
2250	2.54		4.46	
2500	2.25		5.92	
2750	2.15		7.84	
3000	1.99		10.08	
3500	1.61			

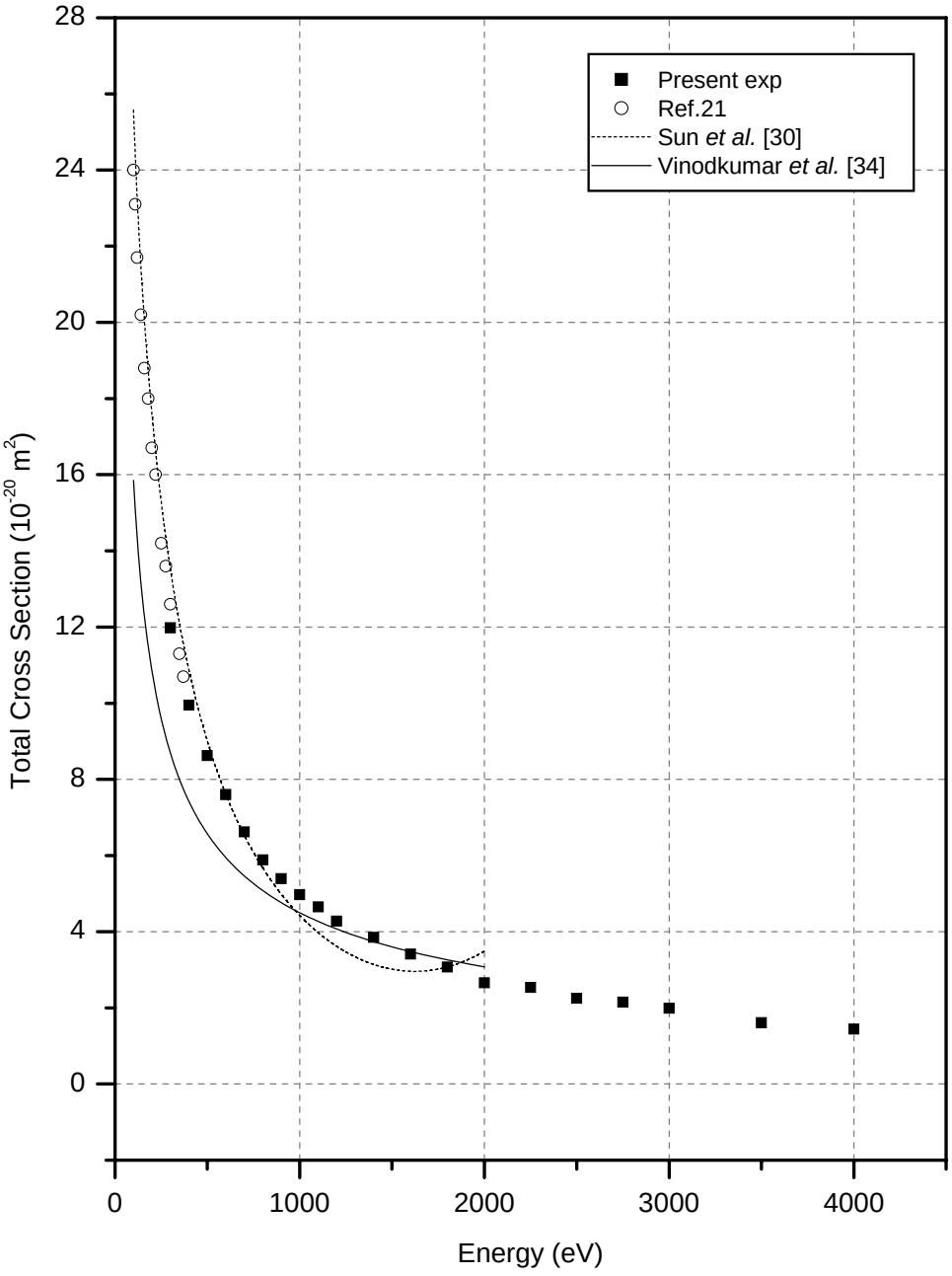

FIG 3.3. Total electron scattering cross sections for C_3H_8 in the units of $10^{-20}\,m^2$ for the energy range 100 to 4000 eV. Squares represent the experimental results of present work and circles represent the experimental cross sections of Szmytkowski and Kwitnewski [21]. Dashed and solid lines are from Sun *et al.* [30] and Vinodkumar *et al.* [34] respectively.

of the present study agree well with the cross sections produced from the theoretical formula of Sun *at al.* [30] up to about 900 eV and at 2000 eV. However their cross sections fall below the present measurements at energies between 1000 and 1800 eV. The deviation of present cross sections from those of Vinodkumar *et al.*[34] is about 0 to 35% in the energy range 100 eV to 1250 eV while they exhibit closer agreement for the energies greater than 1250 eV up to 2000 eV. No theoretical or experimental cross section information was found to compare the present cross sections for the energies higher than 2000 eV.

3.1.2.3 n-Butane, 1,3- Butadiene and Butylene (C_4H_{10}, C_4H_6, C_4H_8) Total electron scattering cross sections for butane, butadiene and butylene have been studied by very few experimental groups only for the lower energies. Floeder *et al.*[12] reported the total cross sections of hydrocarbon targets including C_4H_{10} and C_4H_8 for the energies varying from 100 to 400 eV. Szmytkowski and Kwitnewski [23] measured total cross sections for C_4H_6 in the energy range 0.5 eV to 370 eV. All these studies contain cross sections for lower energies and therefore they are not sufficient to compare the measurements of present study. The total cross section measurements obtained from the present study for these C_4 hydrocarbons are listed in table 3.1 and 3.2 which can be used to identify the patterns of variation of cross sections among each other. Figure 3.4 is a graphical representation of the same facts for a better comparison.

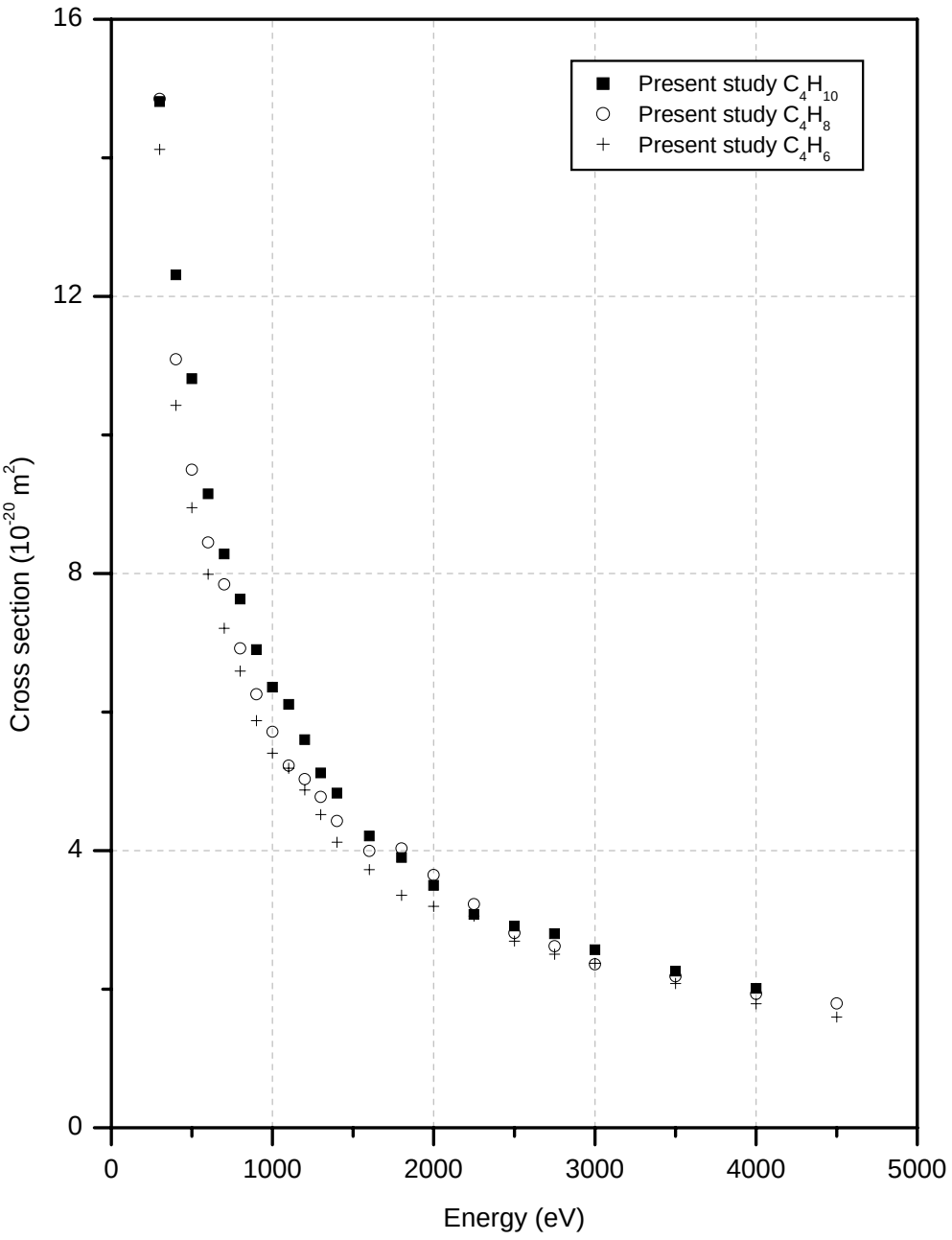

FIG 3.4. The variation of total scattering cross sections with energy for C_4 hydrocarbons. Squares, circles and crosses represent cross sections of C_4H_{10}, C_4H_8 and C_4H_6 respectively.

3.1.3 General Discussion

As can be seen from table 3.2 the electron scattering cross sections for the linear alkanes represented by $C_nH_{2(n+1)}$ increase with the size of the molecule or the number of atoms in the molecule at a constant energy. Each of these molecules represents a same trend against the energy and the cross section is proportional to a negative power of energy as explained by Joshipura and Vinodkumar [26] in the form of Eq (1.2). In general, the total cross section decreases with the decreasing number of hydrogen atoms for C_4 hydrocarbon molecules so that C_4H_{10} has the highest cross section while C_4H_6 has the lowest cross section at a given energy. As shown in Figure 3.4 the differences of cross sections between C_4 hydrocarbons are about 0 % to 10% for the energies less than 1600 eV. These differences of cross sections are negligible for the energies above 1600 eV since the differences are within the experimental error.

3.2 Empirical Formula

3.2.1 Introduction to Empirical Formula

It is very interesting to think of an empirical formula to predict the total cross sections for the linear alkanes represented by $C_nH_{2(n+1)}$ for the energy ranging from 300 eV to 4000 eV specially because of the absence of a successful theoretical model or an empirical model. It is very important to have such an empirical formula because most of the available empirical formulas can be used to construct the cross sections only for lower energies. As mentioned in chapter one, Floeder *et al*. [12] described the measured electron scattering cross sections by a simple formula which is given by equation 1.10 for several hydrocarbons including methane, ethane, propane, butane and 1- butene in the

energy range 100 - 400 eV. Other than this Nishimura and Tawara [14] presented a simple formula to determine the cross sections for intermediate energies, which is given by equation 1.11. This is applicable for hydrocarbon molecules such as CH_4,C_2H_2,C_2H_4, C_2H_6 and C_3H_8 in the energy range 4 – 500 eV. However our aim was to develop a simple empirical formula which is capable of calculating cross sections for linear alkanes, in terms of well known molecular properties. This will be constructed by analyzing the experimental cross sections for C_2H_6, C_3H_8 and C_4H_{10} obtained from the present study and cross sections for CH_4 which obtained from a previous study [43] done in the same laboratory. Furthermore the cross sections for C_4H_6 and C_4H_8 will also be used to identify the trends of cross sections with number of H atoms. Some of the theoretical approaches explained in chapter one will also be used in the construction of present empirical formula. The procedure of construction of empirical formula and results will be discussed in next few sections. The cross sections constructed using this formula will also be compared to the available experimental and theoretical cross sections.

3.2.2 Approach

According to the Joshipura and Vinodkumar [26], the total scattering cross section (σ) in the units of Bohr radius square (a_0^2) for an atom or molecule can be given by Eq 1.2 which is $\sigma = AE^{-B}$, where E is the energy of the electrons in units of keV, A and B are two fitting parameters which can be determine by the molecular properties of the target gas. Equation 1.2 exhibits a linear relationship in between $\ln(\sigma)$ and $\ln(E)$. The experimental cross sections available for the molecules CH_4, C_2H_6, C_3H_8, and C_4H_{10} were plotted in the logarithmic form to compare them with the model given by Joshipura

and Vinodkumar. These plots are displayed in Figures 3.5 to 3.9.

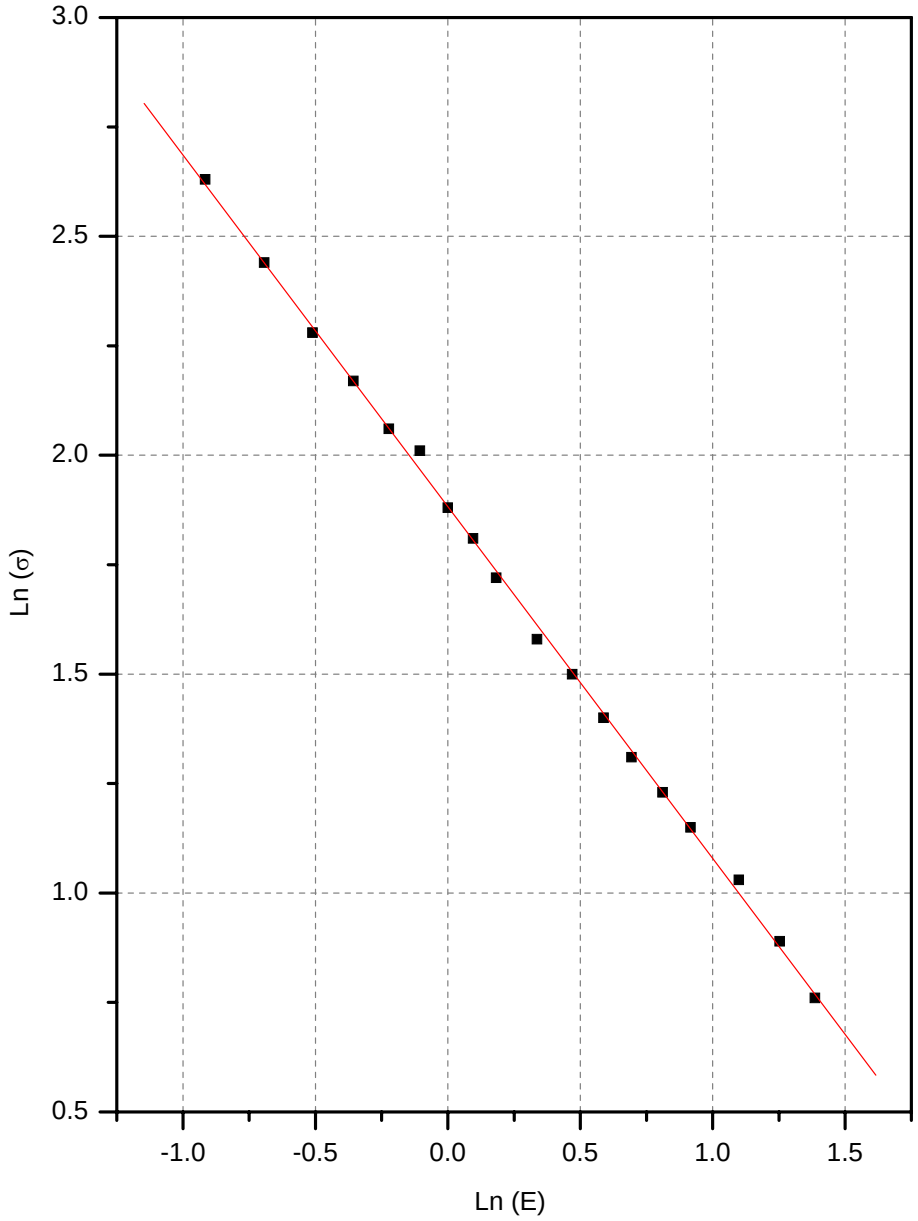

FIG 3.5. Total electron scattering cross sections for CH_4 against energy for the energy range 0.3 to 4.0 keV . Energy is in units of keV and cross section (σ) is in $a_0^{\,2}$ where a_0 is Bohr radius. The solid line is the best fit for experimental data.

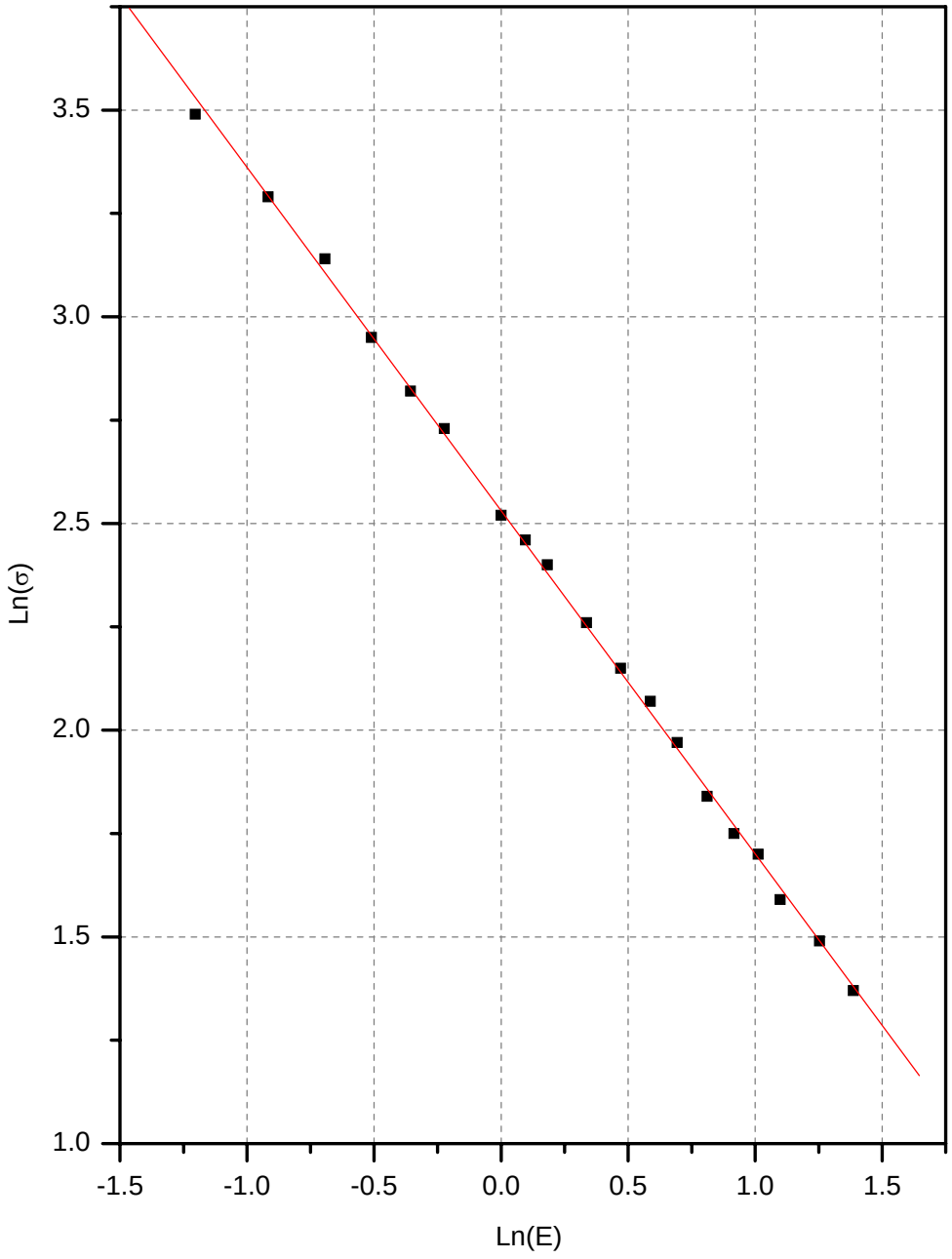

FIG 3.6. Total electron scattering cross sections for C_2H_6 against energy for the energy range 0.3 to 4.0 keV . Energy is in units of keV and cross section (σ) is in $a_0^{\ 2}$ where a_0 is Bohr radius. The solid line is the best fit for experimental data.

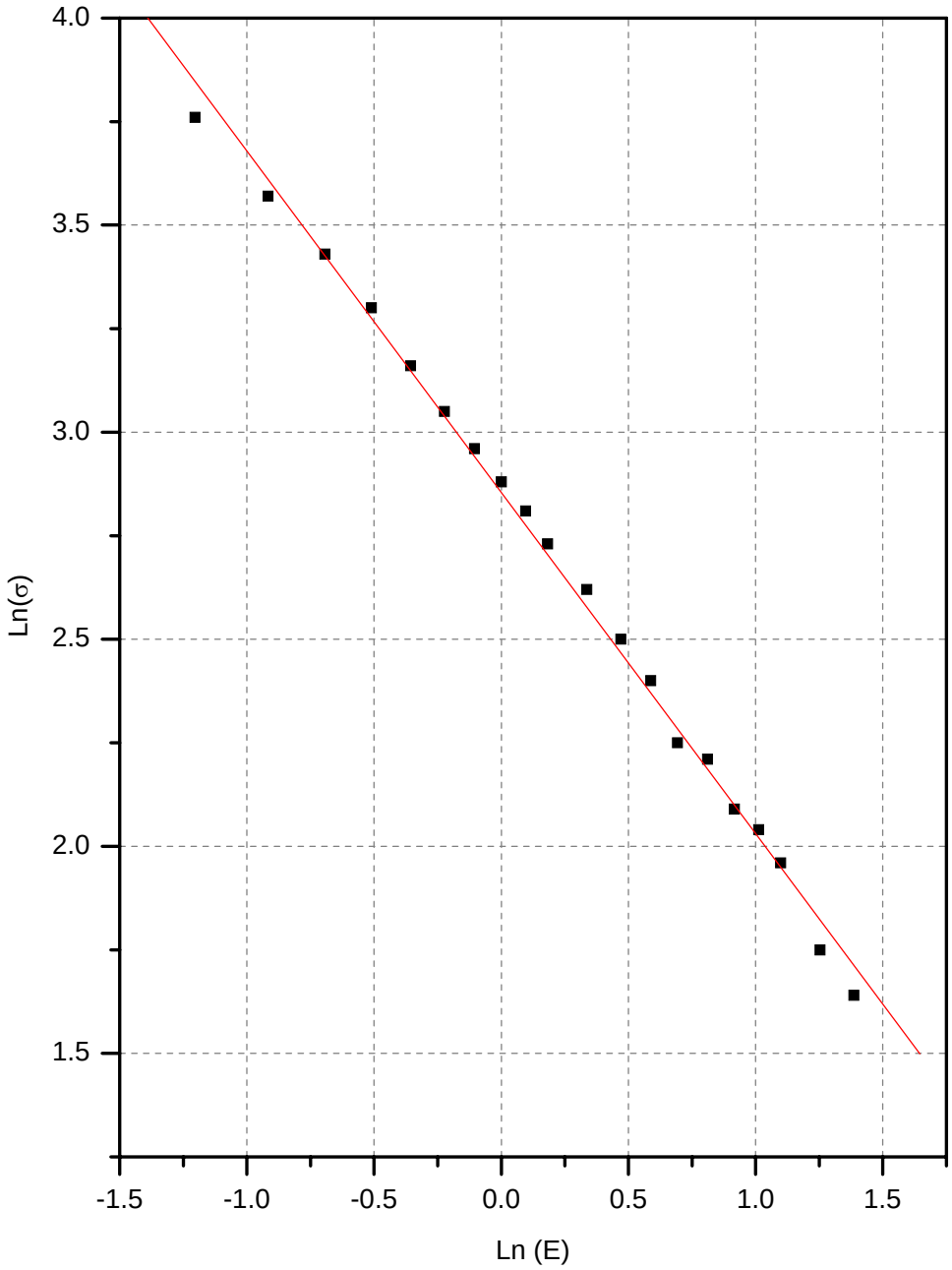

FIG 3.7. Total electron scattering cross sections for C_3H_8 against energy for the energy range 0.3 to 4.0 keV . Energy is in units of keV and cross section (σ) is in $a_0^{\,2}$ where a_0 is Bohr radius. The solid line is the best fit for experimental data.

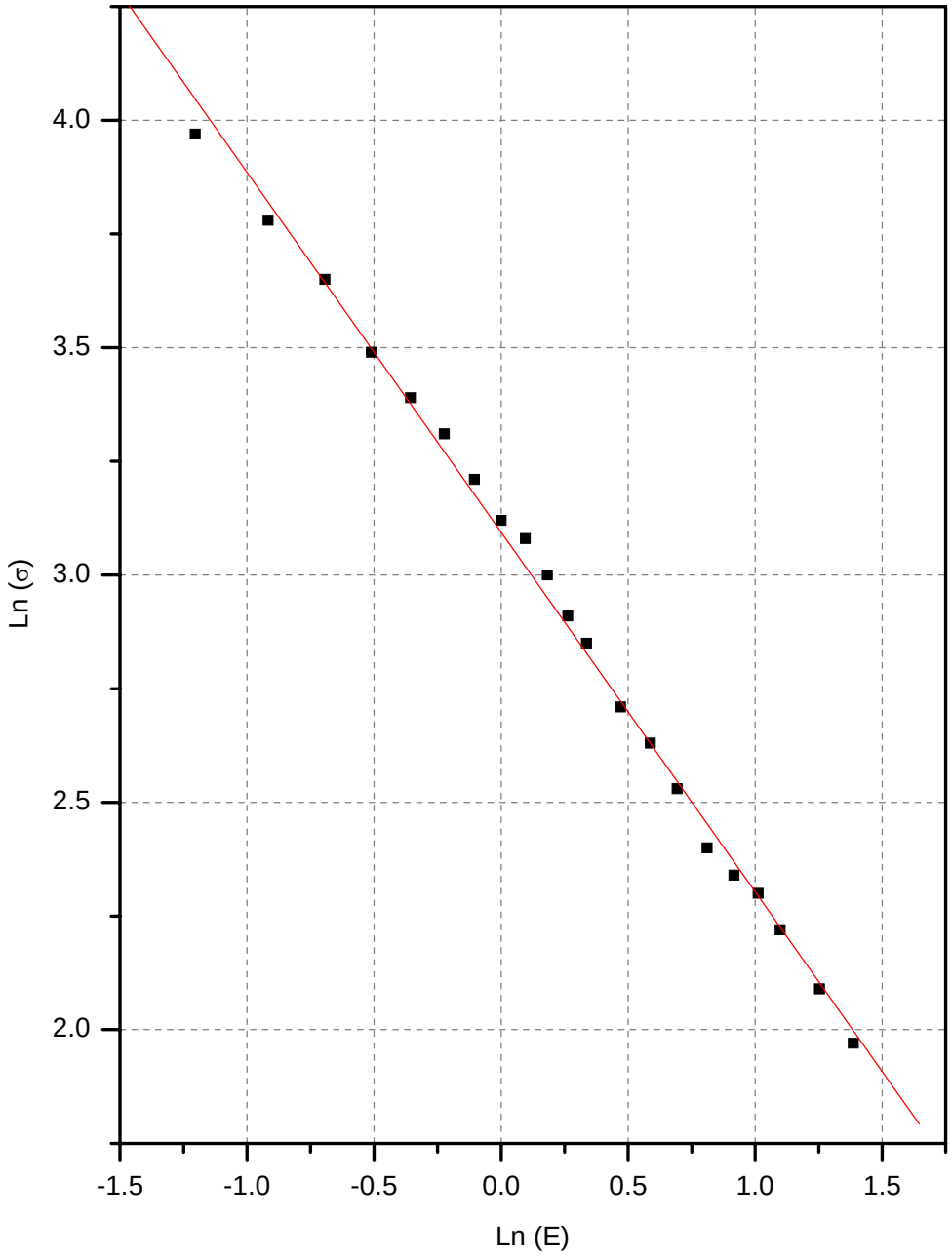

FIG 3.8. Total electron scattering cross sections for C_4H_{10} against energy for the energy range 0.3 to 4.0 keV . Energy is in units of keV and cross section (σ) is in $a_0^{\,2}$ where a_0 is Bohr radius. The solid line is the best fit for experimental data.

Each plot in these figures represents a linear relationship between $\ln(\sigma)$ and $\ln(E)$ and this verifies that the experimental cross sections obtained in the present work along with cross sections for CH_4 from Ref. 43 agree well with the formalism proposed by Joshipura and Vinodkumar [26].

Several authors have stressed the fact that, at a given energy, the total scattering cross section increases with the increasing number of target electrons (Z). Thus the total cross section is also linearly increases with the number of carbon and hydrogen atoms in the molecule. Considering these information the total electron scattering cross section σ for the linear alkanes represented by $C_nH_{2(n+1)}$ (n=1..4) can be defined as,

$$\sigma = a\ N_H + b\ N_C \tag{3.1}$$

where N_H and N_c are the number of hydrogen atoms and the number of carbon atoms in the target molecule while "*a*"and "*b*" are respectively, the cross section of a single hydrogen (H) atom and a single carbon (C) atom at a particular energy. The two terms, "*a*" and "*b*", can be determined using the experimental cross sections of CH_4, C_2H_6, C_3H_8, and C_4H_{10}. The procedure which carried out to evaluate "*a*" and "*b*" will be discussed in the next section.

3.2.3 Methodology

As mentioned in a previous section, the alkanes represented by $C_nH_{2(n+1)}$ show increase in the cross sections with *n*, which can be due to the addition of CH_2 group. Therefore the cross section for CH_2 was calculated first by taking the difference between the two adjacent alkanes for certain energy. In other words, the average cross section for CH_2 was calculated by averaging the values obtained by, $\sigma(C_2H_6) - \sigma(CH_4)$,

$\sigma(C_3H_8)-\sigma(C_2H_6)$ and $\sigma(C_4H_{10})-\sigma(C_3H_8)$ for a specific energy. Then the cross section for H_2 was calculated by using, $\sigma(2H)=\sigma(C_nH_{2(n+1)})-n[\sigma(CH_2)]$ for $n = 1,2,3,4$. $\sigma(C_nH_{2(n+1)})$ is the cross section of the respective alkane given by $C_nH_{2(n+1)}$. The average cross section for 2H was evaluated from it and therefore the cross section for a single H atom in a hydrocarbon molecule, for a given energy can be determined in this manner. Thus having the average cross sections for H and CH_2, The cross section for a single carbon atom can be calculated for certain energy, by simply taking the difference of those. Following the same procedure, the cross section for individual H and C atoms in the molecule can be calculated for energies ranging from 0.3 to 4.0 keV.

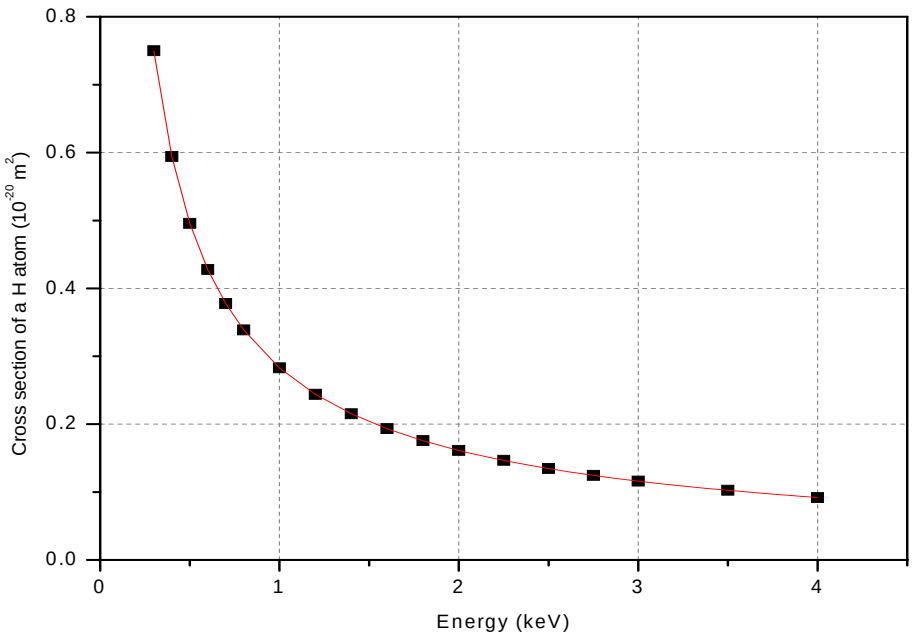

FIG 3.9. The variation of electron scattering cross sections of single H atom in a linear alkane against energy, for the energy range 0.3 to 4.0 keV . Solid line is the best fit for the plotted data.

The variation of cross sections of a single H and a single C atom with energy was then studied. Figure 3.9 represents the variation of the cross section of a single H atom against the energy ranging from 300 eV to 4000 eV. Figure 3.10 represents the same variation for a single C atom.

Both the variations of cross section of H and C atoms with energy, agree with the model defined by Joshipura and Vinodkumar [26] which is given in equation 1.2. The two constants in the equation 1.2 are determined for H by taking the best fit for the plot given in Figure 3.9. This fit represents the energy variation of the term "*a*"in the equation 3.1. Similar procedure was followed in the determination of the energy variation of parameter "*b*" in equation 3.1.

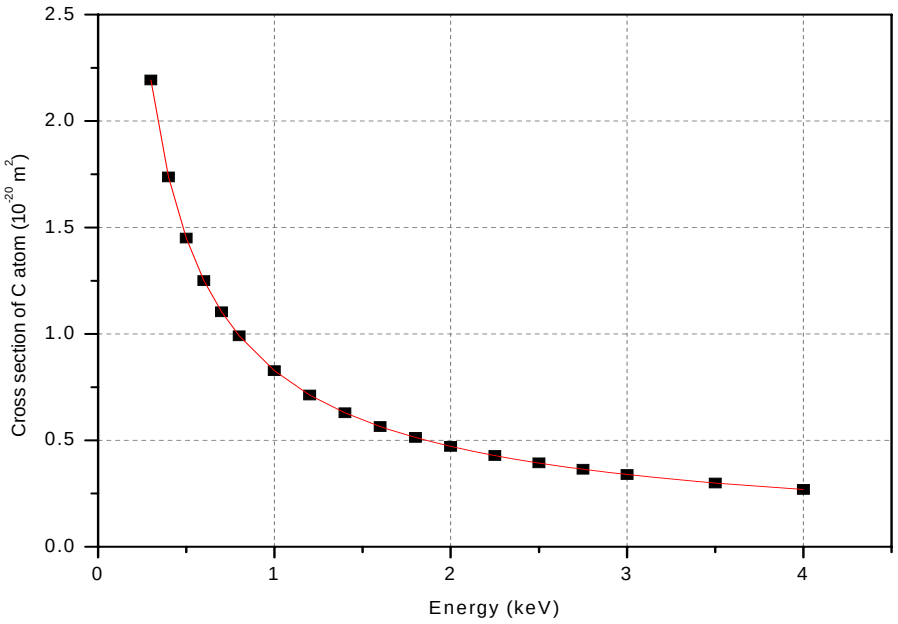

FIG 3.10. The variation of electron scattering cross sections of single C atom in a linear alkane against energy, for the energy range 0.3 to 4.0 keV. Solid line is the best fit for the plotted data.

3.2.4 Results

The procedure explained in the previous section was carried out to evaluate "*a*" and "*b*"in the equation 3.1. The term "*a*", which is the cross section of individual H atom in linear alkanes represented by $C_nH_{2(n+1)}$ (n =1,2,3,4) is evaluated to be ,

$$a = (0.28)\, E^{-0.81} \tag{3.2}$$

where *E* is the energy of the electrons in units of keV. Similarly the term "*b*" in equation 3.1, which is the cross section of single C atom in linear alkanes is evaluated to be,

$$b = (0.83)\, E^{-0.81}. \tag{3.3}$$

Using equations 3.1, 3.2 and 3.3 the cross sections $\sigma\left(C_nH_{2(n+1)}\right)$ of alkanes for the energy interval 0.3 to 4.0 keV, can be written as,

$$\sigma\left(C_nH_{2(n+1)}\right) = \left[\left(0.28 \times N_H\right) + \left(0.83 \times N_C\right)\right] E^{-0.81} \qquad (n = 1,2,3,4) \tag{3.4}$$

where, *E* is the energy of the incoming electrons in the units of keV, N_H and N_C are the number of hydrogen and carbon atoms in the alkane respectively.

3.2.5 Comparison with Other Empirical Models and Experimental Cross Sections

The cross sections constructed by the empirical formula explained above are compared to the cross sections determined by several experimental and theoretical studies. Figure 3.11 to 3.14 shows the variation of total cross sections obtained from different studies along with those constructed from the empirical formula given by equation (3.4). As can be seen from these Figures this formula reproduces the experimental cross sections obtained in this laboratory for linear alkanes within 7 %. As can be seen from Figure 3.11, the cross sections predicted by the present empirical formula shows very good agreement with the experimental cross sections reported presented by Ariyasighe, Wijerathne and Palihawadana [43] as well as those reported by

Garcia and Monero [16]. The predicted cross sections from present empirical formula are 10 – 30% higher than the experimental cross sections from Zecca *et al.* [15] with more deviation for the higher energies. The theoretical cross sections calculated by Garcia and Monero [27] under predict the results of present empirical formula for energies between 300eV to 4000 eV and deviation is about 17 % for the energy 300 eV while it is 10% at the energy 4000 eV indicating the decrease of the deviation with increasing energy.

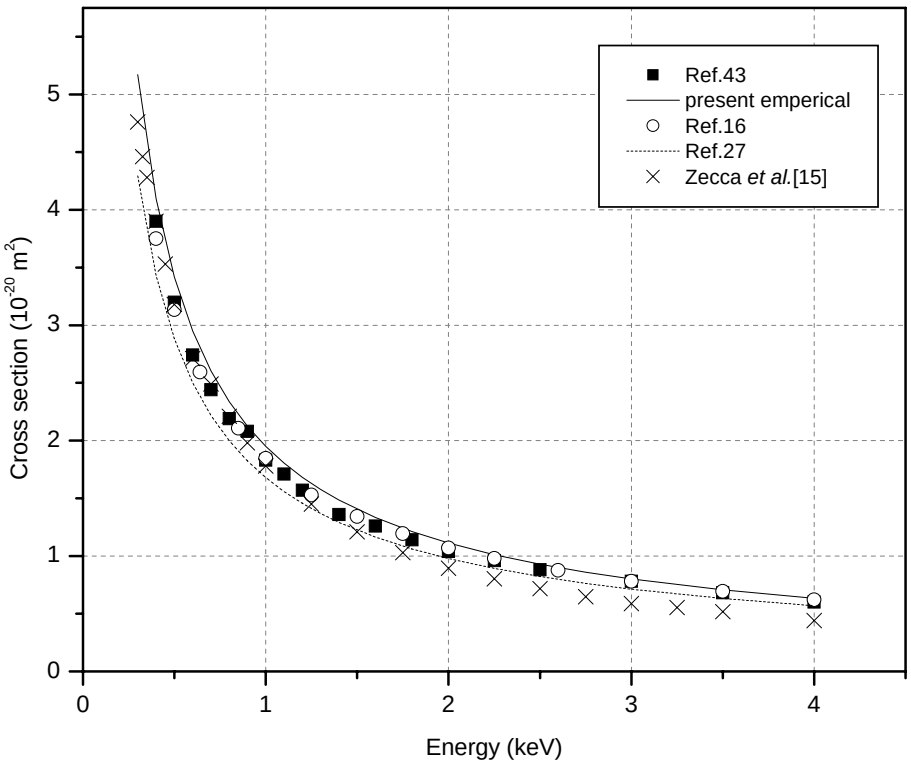

FIG 3.11. Total electron scattering cross sections obtained from available experimental and theoretical studies for CH_4 in the units of $10^{-20}\,m^2$ for the energy range 0.3 to 4.0 keV. The solid line is the predictions from present empirical formula and the dashed line represents the predictions from Garcia and Monero [27] .Squares and circles are the experimental results of Ref.43 and those of Garcia and Monero [16] respectively. Crosses are the experimental cross sections obtained by Zecca *et al.* [15].

Figure 3.12 represents the cross sections produced by the present empirical formula along with those predicted by available experimental and theoretical studies for C_2H_6 at the energies between 0.3 to 4.0 keV.

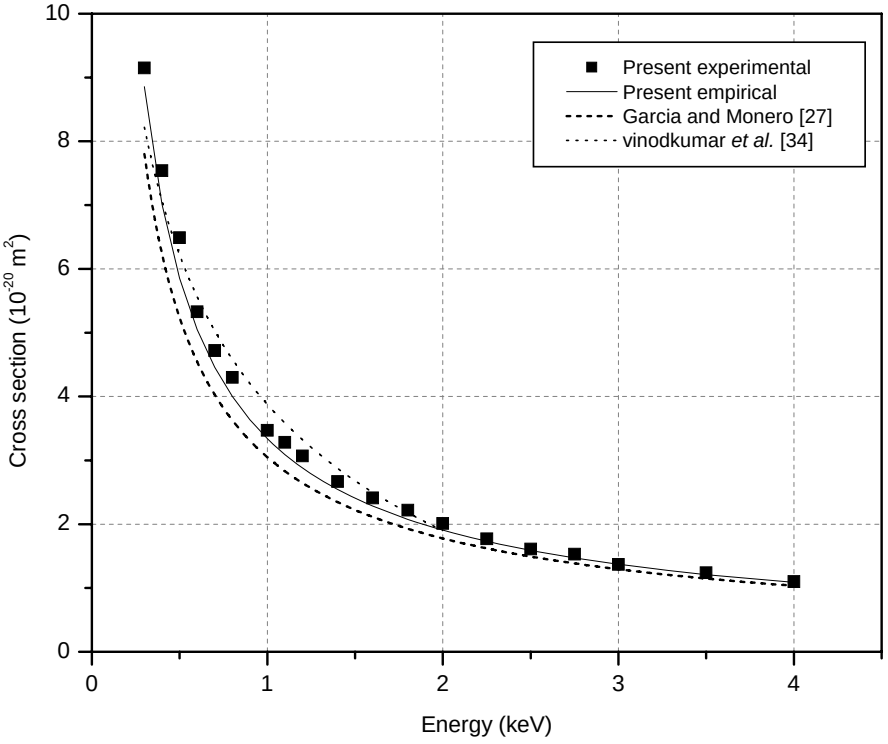

FIG 3.12. Total electron scattering cross sections obtained from available experimental and theoretical studies for C_2H_6 in the units of $10^{-20}\,m^2$ for the energy range 0.3 to 4.0 keV. The solid line is the predictions from present empirical formula and the dashed line represents the predictions from Garcia and Monero [27]. Squares are the present experimental results. Dotted line is the theoretical predictions done by Vinodkumar *et al.* [34].

The values constructed by empirical formula are well agreed with the experimental cross sections obtained from the present study. The theoretical predictions by Vinodkumar *et al.* [34], shows 5 to 20% deviation from the cross sections predicted by the present empirical formula for ethane between 300 eV and 2000 eV energies. As

shown in Figure 3.12, the present cross sections from empirical formula are 7 - 23% higher than those predicted by the Garcia and Monero [27] in the energy range 300 – 2000 eV . However the deviation between them decreases as energy increases and there is only 5% difference between present empirical cross sections and those of Garcia and Monero [27] at energy 4000 eV.

The calculated cross sections using new empirical formula and the experimental cross sections from the present study as well as the cross sections obtained from past studies for the molecule C_3H_8 are presented in Figure 3.13. The experimental cross sections measured in the present study for C_3H_8 falls within 7% of the cross sections produced by present empirical formula for energy 300 eV to 4000 eV.

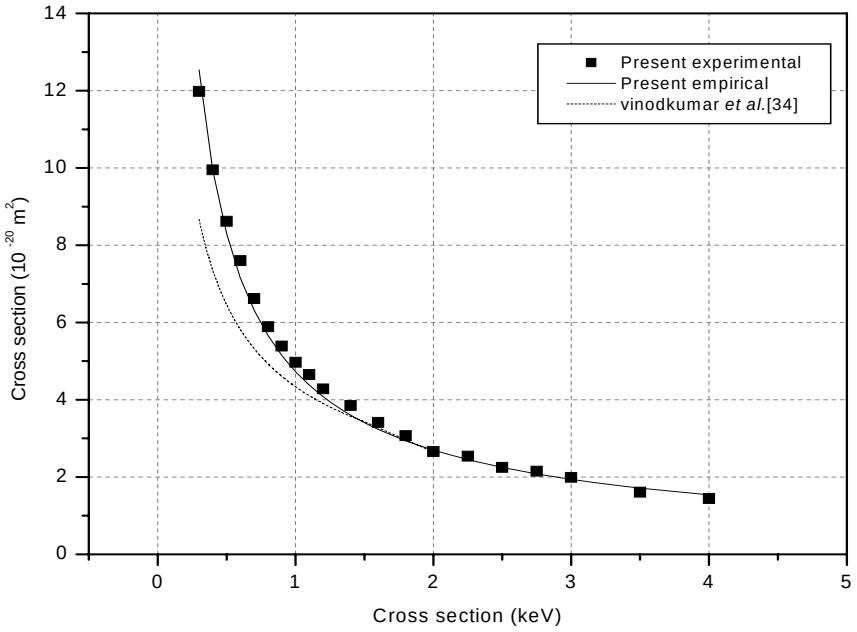

FIG 3.13. Total electron scattering cross sections obtained from available experimental and theoretical studies for C_3H_8 in the units of $10^{-20}\,m^2$ for the energy range 0.3 to 4.0 keV. The solid line is the predictions from present empirical formula and the dashed line represents the predictions from Vinodkumar *et al.* [34]. Squares are the present experimental results.

The cross sections determined by the present empirical formula, are in good agreement with those of Vinodkumar for the energy from about 1400 eV to 2000 eV. There are about 0 - 30% differences between the cross sections of Vinodkumar and those predicted by model for the energy 300 eV to 1400 eV with greater deviations for the lower energies.

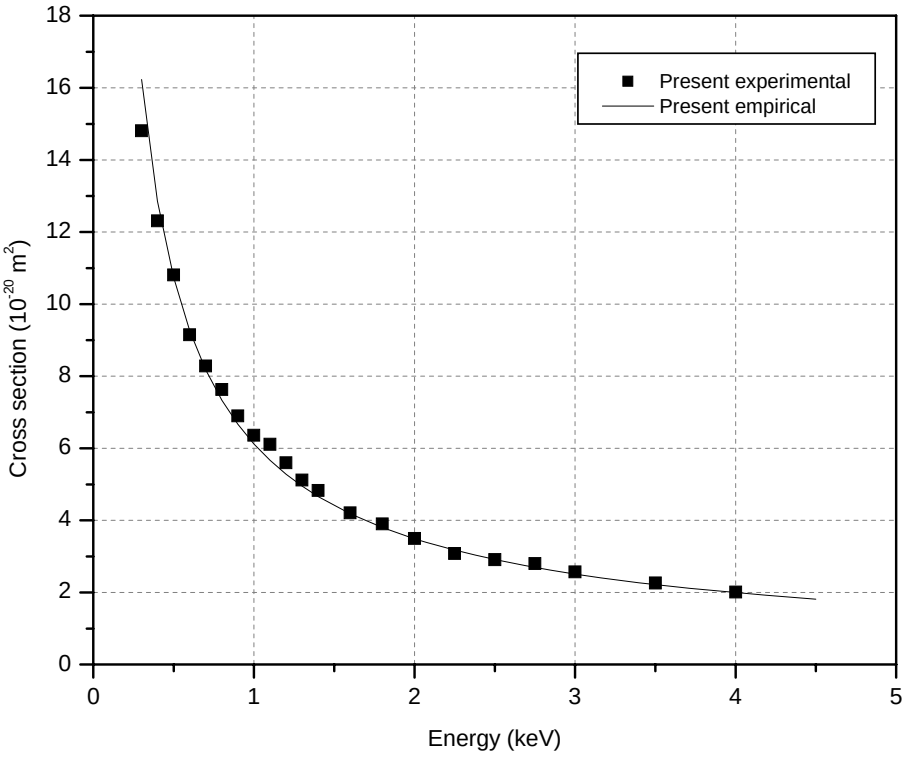

FIG 3.14. Total electron scattering cross sections obtained from available experimental and theoretical studies for C_4H_{10} in the units of $10^{-20}\,m^2$ for the energy range 0.3 to 4.0 keV. The solid line is the predictions from present empirical formula while the squares are the present experimental results.

According to my knowledge, there are no experimental or theoretical total cross sections available in the literature for C_4H_{10} from energy 0.3 to 4.0 keV to compare with

the results of the present study. Therefore the cross sections evaluated by the empirical formula developed here are presented in Figure 3.14 along with the experimental cross sections of the present study. As mentioned earlier they are well agreed within 7% in between 300 – 4000 eV of energy except for 0.3 eV and 1.1 keV energies.

The empirical formula developed here was also used to construct the cross sections for the C_4H_8 and C_4H_6 molecules to check the capability of using this formula for non alkane molecules. Figure 3.15 represents the variations of experimental cross sections for C_4H_6 and C_4H_8 molecules along with those constructed by the empirical formula given in Eq 3.4. As can be seen from the Figure 3.15, the cross sections produced by the empirical formula for C_4H_8 show closer agreement to those measured experimentally. The empirical values reproduce the experimental cross sections for C_4H_8 within 8% in the energy range of 0.3 – 4.5 keV, except for three energy values. The cross sections obtained using the empirical formula underpredict the experimental cross sections of C_4H_6 molecule in the energy range 0.5 – 4.5 keV. The deviation between these two varies within 0 - 16%. These percentage differences between the cross sections produced by empirical formula and those measured experimentally are considered to be high since the experimental cross sections of C_4H_8 and C_4H_6 are very closer to each other. Therefore the cross sections for the hydrocarbon molecules which are having double or triple bonds cannot be predicted accurately using the present empirical formula. The formula introduced here can be corrected to produce cross sections of C_4H_8 and C_4H_6 by adding a suitable correction factor. This correction factor can be evaluated by analyzing the cross sections of different hydrocarbons which are having double and triple carbon – carbon bonds.

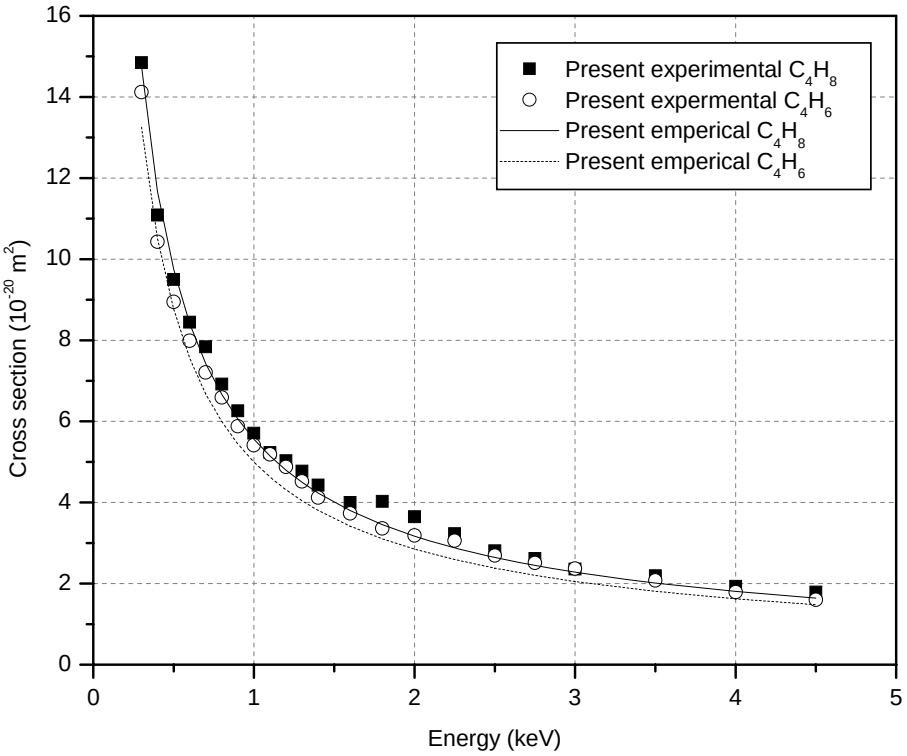

FIG 3.15. Total electron scattering cross sections obtained from present empirical formula along with experimental data for C_4H_8 and C_4H_6 in the units of $10^{-20}\,m^2$ for the energy range 0.3 to 4.5 keV. Solid and dashed lines are the predictions from present empirical formula for C_4H_8 and C_4H_6 respectively. Squares and circles are the present experimental results for C_4H_8 and C_4H_6.

CHAPTER FOUR

Conclusions

The total electron scattering cross sections for C_2H_6, C_3H_8, C_4H_{10}, C_4H_8 and C_4H_6 were determined experimentally using linear transmission technique. The total electron scattering cross sections of these hydrocarbon targets were measured in this study for the intermediate energies varying from 300 to 4000 eV. This completes the available total cross sections for the alkanes represented by $C_nH_{2(n+1)}$ (where n=1, 2, 3, 4) for the energy up to 4000 eV. The present experimental cross sections measured for C_2H_6 and C_3H_8 exhibit closer agreement with the available theoretical and experimental cross sections. The total scattering cross sections for C_4H_8 and C_4H_6 were also studied using same technique for the energy range 300 to 4500 eV. The experimental cross sections studied here for C_4 hydrocarbons are more important because there is no detailed study available in the literature for these molecules for intermediate energies.

A simple empirical formula to predict cross sections was developed by analyzing the present and existing experimental cross sections for alkanes. The cross sections calculated using the present empirical formula are compared with the cross sections obtained by other experimental and theoretical groups as well as the experimental results obtained in the present study. They showed good agreement with the results of recent studies. Therefore the empirical formula developed in the present study can be used to construct accurate total cross sections of linear alkanes up to C_4H_{10} within the energy range 0.3 to 4.0 keV.

REFERENCES

[1] Christophorou L. G., *Electron-Molecule Interactions and Their Applications*, (Academic, Florida, 1984).

[2] Mason N. J, Gingell J. M, Jones N. C, Kamiski L, Phil. Trans.R Soc. Lond A **357** 1175-1200 (1999).

[3] Alman D. A, Ruzic D N, Brooks J N, Phys. Plasmas, **7** , 5 (2000).

[4] Kurt H. Becker, C William McCurdy, Thomas M. Ornaldo, work shop on *Electron driven processes: scientific Challenges and Technological opportunities*, Stevens Institute of Technology.(March ,2000).

[5] Final Report of work shop on, *Research Needs and Opportunities in Radiation Chemistry*, Indian oaks Conference Center, Chesterton, Indiana. (April, 1998).

[6] B. Boudaïffa, P. Cloutier, D. Hunting, M. A. Huels, and L. Sanche, Science **287**, 1658 (2000).

[7] Brode R. B. Phys. Rev. **25** 636-644 (1925).

[8] Bruche E. Ann. Phys. Lpz. **83** 1065 (1927).

[9] Ramseur C. and Kollath R. Ann. Phys. Lpz. **4** 98-108 (1930).

[10] Hasted J. B, Kadifachi S. and Solovyev T. XI Int. conf. on *The Physics of electronic and Atomic and collisions*, Kyoto, Japan, Abstract of of contributed papers, pp. 334-335 (1979).

[11] Barbarito E, Basta M and Calicchio M., J. Chem. Phys. **71** 54-59 (1979).

[12] Floeder K. , Fromme D. , Raith W., Schwab A. , Sinapius G., J. Phys. B: At. Mol. Phys. **18**, 3347-3359 (1985).

[13] Sueoka O. and Mori S. J. Phys. B: At Mol. Opt. Phys. **19** 4035-4050 (1986).

[14] Nishimura H., Tawara H, J. Phys. B: At Mol. Opt. Phys. **24** L363-L366 (1991).

[15] Zecca A., Karwasz G., Brusa R. S., Szmytkowski C. J. Phys. B: At Mol. Opt. Phys. **24** 2747-2754 (1991).

[16] G. Garcia and F. Manero, Phys. Rev. A **57**, 1069-1073 (1998).

[17] Xing S. L., Shi Q. C., Chen X. J., Xu K. Z., Yang B. X., Wu S. L. and Feng R. F. Phys. Rev. A **51**, 414 – 417 (1995).

[18] Tanaka H., Tachibana Y., Kitajima M., Sueoka O., Takaki H. , Hamada A. and Kimura M. Phys. Rev. A **59**, 2006-2015 (1999).

[19] Sanches I. P., Pinto P.R and Iga I., International Symposium on, *Electron-Molecule Collisions and Swarms*, Campinas, SP, Brazil., p. 65 , (July 2005).

[20] W. M. Ariyasinghe and D. Powers, Phys. Rev. A **66**, 052716 (2002).

[21] Szmytkowski C. and Kwitnewski J. Phys. B: At Mol. Opt. Phys. **35** 2613-2623 (2002).

[22] Szmytkowski C. and Kwitnewski J. Phys. B: At Mol. Opt. Phys. **35** 3781-3790 (2002).

[23] Szmytkowski C. and Kwitnewski J. Phys. B: At Mol. Opt. Phys. **36** 2129-2138 (2003).

[24] T. T. Wijerathne, Msc. dissertation, Baylor University, Waco, TX (2004).

[25] Inokuti M. Rev. Mod. Phys. **43** 297 (1971).

[26] K. N. Joshipura, Vinodkumar M., Pramana **47**, 57 (1996).

[27] Garcia G. , Monero F. , Chem. Phys. Lett. **280**, 419 (1997).

[28] Jiang Y. , Sun J., Wan L., Phys. Rev. A **52**, 398 (1995).

[29] Jiang Y. , Sun J., Wan L., J. Phys. B: At Mol. Opt. Phys. **30** 5025-5032 (1997).

[30] Sun J., Du C. , Shi D., Liu Y. Chin.Phys. Soc. **13,** 1418(2004).

[31] Joshipura K. N, Vinodkumar M. Phys. Lett. A **224**, 361 (1997).

[32] Joshipura K. N, Vinodkumar M. Eur. Phys. J. D **5**, 299 (1999).

[33] Jiang A. , Baluja K. L , Phys. Rev. A **45**, 202 (1992).

[34] M. Vinodkumar, K. N. Joshipura, C. G. Limbachiya, and B.K Antony, Eur. Phys.J. D **37**, 67-74 (2006).

[35] C. P. Goains, Ph. D. dissertation, Baylor University, Waco, TX (2004).

[36] Kimball Physics EGG-3101, Instruction Manual, Kimball Physics Inc., Wilton, NH.

[37] Kimball Physics EGPS-3101, Instruction Manual, Kimball Physics Inc.,Wilton, NH.

[38] MKS Baratron 626 A, Capacitance Manometer, Instructions Manual, MKS Instruments, Andover, Massachusetts.

[39] Kiethley model 480 picoammeter, Instruction Manual, Keithly Inc.

[40] Ametek Dycor model Quadrapole gas Analyzer, Instructions Manual, Ametek Process Instruments, Pittsburgh, PA.

[41] W. M. Ariyasinghe, T. Wijerathna and D. Powers, Phys. Rev. A **68**, 032708 (2003).

[42] P. Guo, A. Ghebremedhin,W. M. Ariyasinghe and D. Powers, Phys. Rev. A **51**, 2117 (1995).

[43] W. M. Ariyasinghe, T. Wijerathna and P. Palihawadana, Nucl. Instrm. Methods Phys. Res. B 217, 389-395 (2003).

BIBILIOGRAPHY

Alman D. A, Ruzic D N, Brooks J N, Phys. Plasmas, **7** , 5 (2000)

Ametek Dycor model Quadrapole gas Analyzer, Instructions Manual, Ametek Thermox.

Ariyasinghe W. M. and Powers D., Phys. Rev. A **66**, 052716 (2002).

Ariyasinghe W. M., Wijerathna T. and Palihawadana P., NIMB. . B 217, 389-395 (2003).

Ariyasinghe W. M., Wijerathna T. and Powers D., Phys. Rev. A **68**, 032708 (2003).

Barbarito E, Basta M and Calicchio M., J. Chem. Phys. **71** 54-59 (1979)

Boudaïffa B., Cloutier P., Hunting D., Huels M. A., and Sanche L., Science **287**, 1658 (2000).

Brode R. B. Phys. Rev. **25** 636-644 (1925)

Bruche E. Ann. Phys. Lpz. **83** 1065 (1927)

Christophorou L. G., *Electron-Molecule Interactions and Their Applications*, (Academic,Florida, 1984).

Final Report of work shop on, *Research Needs and Opportunities in Radiation Chemistry*, Indian oaks Conference Center, Chesterton, Indiana. (April, 1998)

Floeder K. , Fromme D. , Raith W., Schwab A. , Sinapius G., J. Phys. B: At. Mol. Phys. **18**, 3347-3359 (1985).

Garcia G. and Manero F., Phys. Rev. A **57**, 1069-1073 (1998).

Garcia G. , Monero F. , Chem. Phys. Lett. **280**, 419 (1997)

Goains C. P., Ph. D. dissertation, Baylor University, Waco, TX (2004).

Guo P., Ghebremedhin A., Ariyasinghe W. M. and Powers D., Phys. Rev. A **51**, 2117 (1995).

Hasted J. B, Kadifachi S. and Solovyev T. XI Int. conf. on the Physics of electronic and Atomic and collisions, Kyoto, Japan, Abstract of of contributed papers, pp. 334-335 (1979)

Inokuti M. Rev. Mod. Phys. **43** 297 (1971)

Jiang A. , Baluja K. L , Phys. Rev. A **45**, 202 (1992)

Jiang Y. , Sun J., Wan L., J. Phys. B: At Mol. Opt. Phys. **30** 5025-5032 (1997)

Jiang Y. , Sun J., Wan L., Phys. Rev. A **52**, 398 (1995)

Joshipura K. N, Vinodkumar M. Eur. Phys. J. D **5**, 299 (1999)

Joshipura K. N, Vinodkumar M. Phys. Lett. A **224**, 361 (1997)

Joshipura K. N., Vinodkumar M., J. Phys. Pramana 47, 57 (1996).

Kiethley model 480 picoammeter, Instruction Manual, Keithly Inc.

Kimball Physics EGG-3101 , Instruction Manual, Kimball Physics Inc.

Kimball Physics EGPS-3101, Instruction Manual, Kimball Physics Inc.

Kurt H. Becker, C William McCurdy, Thomas M. Ornaldo, work shop on *Electron driven processes: scientific Challenges and Technological opportunities*, Stevens Institute of Technology.(March ,2000)

Mason N. J, Gingell J. M, Jones N. C, Kamiski L, Phil. Trans.R Soc. Lond A **357** 1175-1200 (1999)

MKS Baratron 626 A, Capacitance Manometer, Instructions Manual, MKS Instruments.

Nishimura H., Tawara H, J. Phys. B: At Mol. Opt. Phys. **24** L363-L366 (1991)

Ramseur C. and Kollath R. Ann. Phys. Lpz. **4** 98-108 (1930)

Sanches I. P., Pinto P.R and Iga I., International Symposium on, *Electron-Molecule Collisions and Swarms*, Campinas, SP, Brazil., p. 65 , (July 2005)

Sueoka O. and Mori S. J. Phys. B: At Mol. Opt. Phys. **19** 4035-4050 (1986)

Sun J., Du C. , Shi D. Liu Y. Chin.Phys. Soc. **13,** 1418(2004)

Szmytkowski C. and Kwitnewski J. Phys. B: At Mol. Opt. Phys. **35** 2613-2623 (2002)

Szmytkowski C. and Kwitnewski J. Phys. B: At Mol. Opt. Phys. **35** 3781-3790 (2002)

Szmytkowski C. and Kwitnewski J. Phys. B: At Mol. Opt. Phys. **36** 2129-2138

Tanaka H., Tachibana Y., Kitajima M., Sueoka O., Takaki H. , Hamada A. and Kimura M. Phys. Rev. A **59**, 2006-2015 (1999).

Vinodkumar M., K. N. Joshipura, C. G. Limbachiya, and B.K Antony, Eur. Phys.J. D **37**, 67-74 (2006)

Wijerathne T. T., Msc. dissertation, Baylor University, Waco, TX (2004).

Xing S. L., Shi Q. C., Chen X. J., Xu K. Z., Yang B. X., Wu S. L. and Feng R. F. Phys. Rev. A **51**, 414 – 417 (1995).

Zecca A., Karwasz G., Brusa R. S., Szmytkowski C. J. Phys. B: At Mol. Opt. Phys. **24** 2747-2754 (1991).